1-1-2023

Event-Based Robust Control Techniques for Wheel-Based Robots Under Cyber-Attack and Dynamic Quantizer

Mobin Saeedi
Shiraz University of Technology

Jafar Zarei
Shiraz University of Technology

Mehrdad Saif
University of Windsor

Allahyar Montazeri
Lancaster University

Event-Based Robust Control Techniques for Wheel-Based Robots Under Cyber-Attack and Dynamic Quantizer

Mobin Saeedi, Jafar Zarei, Mehrdad Saif, and Allahyar Montazeri

Abstract Nowadays, mobile robots are becoming an increasingly significant part of daily human life. Humanoid robots, wheeled mobile robots, aerial vehicles, mobile manipulators, and more are examples of mobile robots. As opposed to other robots, they are capable of moving autonomously, with sufficient intelligence to make decisions in response to the perceptions they receive from their environment. In today's world, cooperative tasks and the ability to control robots via networks make them a component of cyber-physical systems (CPSs). In this study, mobile robots that are acting as a part of CPSs are examined. Data-network burden, signal quantizers, cyber security, delayed transition, and robust performance are some of the challenges they face. A total of three sections are then devoted to addressing these issues in detail. As a first step, the governing equation for mobile robots is explained, and then their robust and resilient behavior of them is examined by establishing the event-triggered adaptive optimal terminal sliding mode control (AOTSMC) approach for nonlinear uncertain dynamic systems that are subjected to denial-of-service (DoS) cyber attacks. In this case, it is assumed that the conveyed signal is being corrupted randomly by an attacker. In this situation, it is essential to design the closed-loop controller parameters in such a way that the performance can be maintained under malicious attacks while the communication resources are preserved. Due to the unrealistic nature of delayed-free communication, the stability analysis is conducted for a general form of uncertain nonlinear delayed input dynamic systems. The quantization effect on the closed-loop control system is then analyzed in conjunction with

M. Saeedi · J. Zarei
Shiraz University of Technology, Shiraz, Iran
e-mail: m.saeedi@sutech.ac.ir

J. Zarei
e-mail: zarei@sutech.ac.ir

M. Saif
University of Windsor, Windsor, ON N9B2M4, Canada
e-mail: msaif@uwindsor.ca

A. Montazeri (✉)
School of Engineering, Lancaster University, Lancaster LA14YW, England
e-mail: a.montazeri@lancaster.ac.uk

A. T. Azar et al. (eds.), *Mobile Robot: Motion Control and Path Planning*,
Studies in Computational Intelligence 1090,
https://doi.org/10.1007/978-3-031-26564-8_6

robust behavior and event-based data transmission. A novel criterion is established to adjust dynamic quantizers' parameters according to the variation of event-triggering error, enabling the quantizer to be more accurate and facilitating implementation procedures. Finally, simulation results validate the presented methodology.

Keywords Mobile robots · Cyber-physical system (CPS) · Event-triggered methodology · Terminal SMC · DoS cyber attack · Dynamic quantizer

1 Introduction

There has been an unstoppable development in cyber-physical systems (CPS) in the engineering field in the last decade. They are constantly under development to become more secure, precise, and capable of making real-time adjustments in the engineering and manufacturing fields. Cyber-based control of robotic mobile devices gives them greater flexibility in terms of their application in different areas of industry, such as warehouse management systems, product assembly, distribution, and hazardous environments [1, 2]. The importance of this issue motivates us to present the current study in which the limitations and considerations of cyber-based mobile robots are addressed. Described in the following two subsections is a review of the CPSs, mobile robots, their dynamic behavior, and their challenges. A typical cyber-based control structure for mobile robots is shown in Fig. 1.

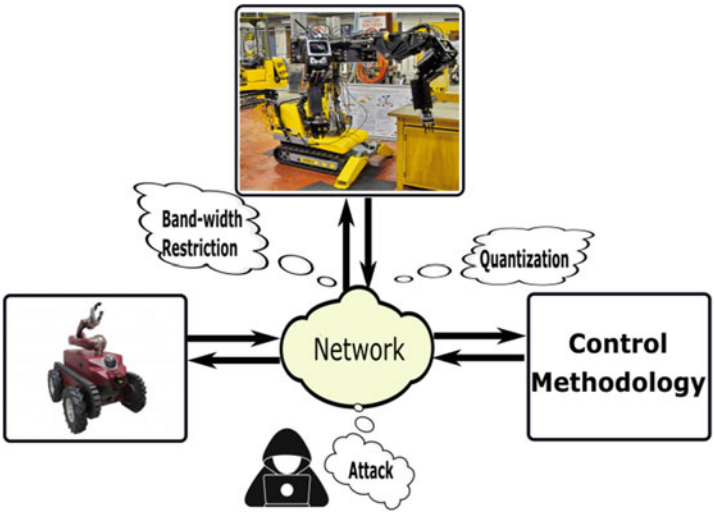

Fig. 1 A typical cyber-based mobile robot control system

1.1 Background

In recent years, there has been a growing interest in CPSs as a result of rapid advancements in digital communications [3]. These new areas require integrating physical systems, microprocessor-based controllers, and sensors through shared cyber layers to achieve desired objectives. As a result of the emergence of such systems, a new research area has emerged that provides control analysis of critical industries, such as oil and gas industry, health care services, as well as the robotic field [4].

Despite the fact that CPS systems offer increased availability and flexibility, there are a number of limitations associated with them, including packet dropout [5, 6], cyber-attacks [7–9], fading data [10], quantization of signals [11–13], and communication delay [14]. Satisfying the limited network bandwidth is an important issue while cyber layer is deployed to transmit data-packets. To cope with this problem, event-triggered data transitions have been developed as an alternative to time-triggered data transitions. Based on the research conducted on the event-triggering schemes, it has been found that it is an effective tool for reducing communication burdens, improving robustness against packet dropouts, and reducing vulnerabilities to cyber attacks [15, 16].

As opposed to traditional time-based methods that cyclically transmit signals within predetermined time instances, an event-triggered terminology would be viewed as a sample-based scheme. There are certain criteria that allow the transmission of measured data at a periodic time intervals that save communication resources while maintaining stability. Although the use of event-based methodology provides an analytical approach to make different control theories applicable to the CPSs in the presence of constraints in the network layer, proving Zeno-free behavior of the designed closed-loop, increased computational load in the design phase [17–21].

When it comes to event-triggering criteria and signal quantization, theory and practice are intertwined in CPSs. It is very important to maintain control precision and stability in physical systems controlled by digital communication, which involves constraints including maximum allowable resolution of analog to digital converters (ADC) [22], quantization errors [23], and the adjustment of sensitivity parameters in dynamic quantizers [24]. It has been shown that most studies by considering certain linear dynamics, present a quantization terminology or demonstrate criteria based on the continuous evolution of the quantizer sensitivity over time [24–26]. Applying these approaches to physical experiments in which time-varying desired responses are included in nonlinear uncertain dynamics does not lead to satisfactory results.

Cyber networks also face a number of challenges when it comes to controlling uncertain dynamic systems. The fulfillment of predefined control tasks for uncertain linear and nonlinear dynamics is always one of the essential researchers' concerns. Then, a lot of robust technics have been established to achieve this target. Among them, one of the most successful control schemes to deal with uncertain dynamic systems is sliding mode control (SMC) approaches [27–29]. Several studies have been conducted in the area of SMC, and various terminologies have been adopted, including event-triggered SMC [25, 30, 31], finite-time convergence [32, 33], switched

systems [20], adaptive control [32, 34, 35], and cyber security [36–38]. Under event-triggering criteria, a super-twisting sliding mode controller is proposed in [19, 39, 40]. A sliding mode controller was developed in [41] for the quadruple-tank multi-input multi-output process with input delay. The terminal sliding mode controller is implemented in [32, 33] to find finite-time convergence.

In this work, the problem of event-triggered terminal SMC (ETSMC) in the presence of a malicious DoS attacks for uncertain nonlinear dynamic systems is investigated. Meanwhile, to consider the quantization problem, the new event-based dynamic quantizer is developed to reach maximum accuracy by adjusting the quantizer sensitivity. The novelty of this work would be categorized as:

- Presenting a new event-based optimal terminal SMC to achieve stability in regulation and tracking tasks for a nonlinear dynamic in the presence of uncertain terms under DoS attacks.
- In order to maintain stability under the presented control scheme despite being attacked by cyber criminals, a unique criterion is developed to take into account the DoS attack characteristics. despite being attacked by cyber criminals.
- A new dynamic quantizer approach in the presence of event-based methodology is provided to achieve stability and accuracy in different practical constraints.

The next subsection investigates the governing dynamic equation of wheeled mobile robots (WMRs).

1.2 Motivations

Throughout the past few decades, a large quantity of investigation is performed on controlling nonholonomic wheeled mobile robots (WMRs). Among the control research topics that have been investigated for nonholonomic systems, the two main problems involved in the research are tracking and stabilization. Taking a look at Kolmanovsky's survey paper [42], one can see the intensive research efforts that are being made in this area. As many researchers have shown [43], stabilizing the equilibrium point of is a difficult problem due to structure of the governing differential equations. Since nonholonomic systems such as wheeled mobile robots, do not satisfy the Brockett condition, the linear control techniques do not provide an effective approach to address this class of systems.

Furthermore, in [44] it is shown that using constant state feedback is not useful in stabilizing nonholomonic systems. As part of the efforts of stabilizing WMRs, several approaches, including discontinuous state feedback [6], time-varying state feedback [45], hybrid controllers [46], and optimal control approaches [47] have been proposed. In fact, majority of methods applied the class of nonholonomic systems successfully are using the concept of chained form to represent the model. There have been a number of control models and strategies developed in order to stabilize uncertain chained systems. In [48], the stabilization problem for nonholonomic

single-chained systems is addressed in the context of nonregular feedback linearization. In [49], the nonholonomic systems with nonlinear drifts are globally stabilized. A robust algorithm for nonholonomic robot control is presented in [50]. However, the primary disadvantage of such works is that they do not consider the dynamics of the system.

Since commercially available wheeled mobile robots do not have velocity sensors, using velocity state feedback is not practical and designing an output feedback controller for nonholonomic wheele-based robots is of practical importance. To solve this critical problem, researchers proposed a global output feedback stabilizing controller for a unicycle-type mobile robot based on the backstepping technique. Although, the majority of the proposed studies suffer from complexity and do not consider uncertain dynamic systems.

In the following subsection equations that represent the dynamic of wheeled mobile robots (WMRs) are formulated. The next sections are devoted to the design of an event-based robust controller in the presence of cyber challenges, such as signal quantization and cyber malicious attacks.

1.3 Problem Statement

Consider the nonholonomic wheeled mobile robot's dynamic as follows,

$$M(\varphi)\,\ddot{\varphi} + B(\varphi)\,\tau_d(t) + C(\varphi,\dot{\varphi})\dot{\varphi} + B(\varphi)\,F(\dot{\varphi}) = B(\varphi)\,\tau - A(\varphi)^T\lambda, \quad (1)$$

and,

$$A(\varphi)\,\dot{\varphi} = 0, \quad (2)$$

where $\varphi = [\varphi_1, \ldots \varphi_n]^T$ is a vector of generalized coordinates, actuators' inputs are defined by $\tau \in \mathbb{R}^{(n-m)\times 1}$ $M(\varphi) \in \mathbb{R}^{n\times n}$ expresses an inertia matrix, the Coriolis matrix is denoted by $C(\varphi,\dot{\varphi}) \in \mathbb{R}^{n\times n}$, friction vector is defined by $F(\dot{\varphi}) \in \mathbb{R}^{(n-m)\times 1}$, and $\tau_d(t) \in \mathbb{R}^{(n-m)\times 1}$ expresses external disturbances, $B(\varphi) \in \mathbb{R}^{n\times(n-m)}$ defines the input transformation matrix. Note that $A(\varphi) \in \mathbb{R}^{m\times n}$ is a full-rank matrix and Lagrange multiplier is expressed by $\lambda \in \mathbb{R}^{m\times 1}$ that denotes constraint forces. Suppose $S(\varphi) = [s_1(\varphi), \ldots, s_{n-m}(\varphi)]^T$, where $s_i(\varphi) \in \mathbb{R}^n$, $i = 1, \ldots, n-m$, and $A(\varphi)S(\varphi) = 0$. The pseudo-velocities of the system can now be obtained by considering (2) as $v(t) = [v_1(t), \ldots, v_{n-m}(t)]^T$ such that

$$\dot{\varphi} = s_1(\varphi)\,v_1 + \cdots + s_{n-m}(\varphi)\,v_{n-m}. \quad (3)$$

Then, by considering (3), (1) can be rewritten as,

$$M_1\dot{v}(t) + C_1(\varphi,\dot{\varphi})\,v(t) + F_1(\dot{\varphi}) + \tau_{d1}(t) = B_1(\varphi)\tau, \quad (4)$$

where $M_1 = S^T(\varphi)M(\varphi)S(\varphi)$, $B_1(\varphi) = S^T(\varphi)B(\varphi)$, $F_1(\dot{\varphi}) = B_1(\varphi)F(\dot{\varphi})$, $\tau_{d1}(t) = B_1(\varphi)\tau_d(t)$, $C_1(\varphi, \dot{\varphi}) = S^T(\varphi)M(\varphi)\dot{S}(\varphi) + S^T(\varphi)C(\varphi, \dot{\varphi})S(\varphi)$.

In order to take actuators dynamic into account, firstly assume that the robot is being operated by $n - m$ DC motors. It is possible to write the electrical equation of each motor armature in the following way,

$$u_a = L_a \frac{di_a}{dt} + k_b \dot{\theta}_m + R_a i_a, \tag{5}$$

where k_b defines the back electromotive force (EMF) constant, L_a, R_a introduce the inductance and resistance of the motor armature, respectively, and the voltage input is defined by u_a. Considering torque and armature current in the absence of armature inductance, i.e. $\tau_m = k_\tau\, i_a$, and pre- and post-gear torque-velocity relationships, i.e. $\tau = n\,\tau_m$ and $\dot{\theta}_m = n\,\dot{\theta}$, the delivered torque to the system can be expressed as,

$$\tau = k_1\, u_a - k_2 \dot{\theta}, \tag{6}$$

where $k_1 = (nk_\tau / R_a)$, and, $k_2 = n\, k_b k_1$, n is gear ratio and k_τ is torque constant of the motor. The Eq. (6) can be represented as follows,

$$\tau = k_1\, u_a - k_2 X_1 v, \tag{7}$$

where $X_1 \in \mathbb{R}^{(n-m)\times(n-m)}$ creates pseudo-velocity vectors from wheels velocities. From (7) and (4), one can obtain,

$$M_1(\varphi)\dot{v}(t) + (C_1(\varphi, \dot{\varphi}) + k_2 B_1(\varphi) X_1(\varphi))\, v(t) + F_1(\dot{\varphi}) + \tau_{d1}(t) = k_1 B_1(\varphi)\, u_a. \tag{8}$$

Note that $M_1(q)$ satisfies inequality $m_1 \leq \|M_1(q)\| \leq m_2$, where m_1 and m_2 are positive scalar constants. The dynamic equation (8) and kinematic model (3) can be defined as follows,

$$\dot{x} = \begin{bmatrix} \dot{\varphi} \\ \dot{v} \end{bmatrix} = \begin{bmatrix} Sv \\ -M_1^{-1}((C_1 + k_2 B_1 X_1)\, v(t) + F_1 + \tau_{d1}) \end{bmatrix} + \begin{bmatrix} 0 \\ k_1 M_1^{-1}\, B_1 \end{bmatrix} u_a, \tag{9}$$

where $x \in \mathbb{R}^{(2n-m)}$ is the state vector. Note that at the rest of this study, the following formulation is dropped to investigate the controller design approach,

$$\dot{x}(t) = f(x(t)) + \Delta f(x(t)) + d(x, t) + bu(t), \tag{10}$$

where $x(t) = [x_1(t), \ldots, x_n(t)]^T \in \mathbb{R}^n$ is the system state, $\Delta f(x(t)) \in \mathbb{R}^n$ represents unknown terms, $d(x, t) \in \mathbb{R}^n$ an external disturbance, $u(t)$ defines input signal, and b is a constant parameter.

1.4 Chapter Organisation

After this introduction, the problem of event-based AOTSMC design in the presence DoS attacks for mobile robots is formulated and solved in Sect. 2. The quantization problem and a solution based on event-triggered terminal SMC design for uncertain input-delayed dynamics are formulated and the numerical results are provided in Sect. 3, and finally conclusions come in Sect. 4.

2 Event-Based AOTSMC Design Under DoS Attacks

An event-triggered adaptive optimal terminal sliding mode control (EAOTSMC) design approach under DoS attacks is presented in this section. Attackers are believed to ruin measurement signals randomly. Maintaining the closed-loop stability under malicious DoS attacks is the most important challenge. In order to achieve this goal, the EAOTSMC has been proposed in order to increase the robustness against attacks and reduce the computational load as a result, as shown in Fig. 2. Furthermore, the frequency and duration of DoS attacks are examined explicitly for their effect on the closed-loop stability, as well as on the schedules for controller updates. Thus, the cyber layer's bandwidth is determined to maintain closed-loop stability. Then, in the presence of uncertainties and DoS attacks, designed parameters can be adjusted by the designer. Finally, an evaluation of the proposed methodology is provided by numerical simulations.

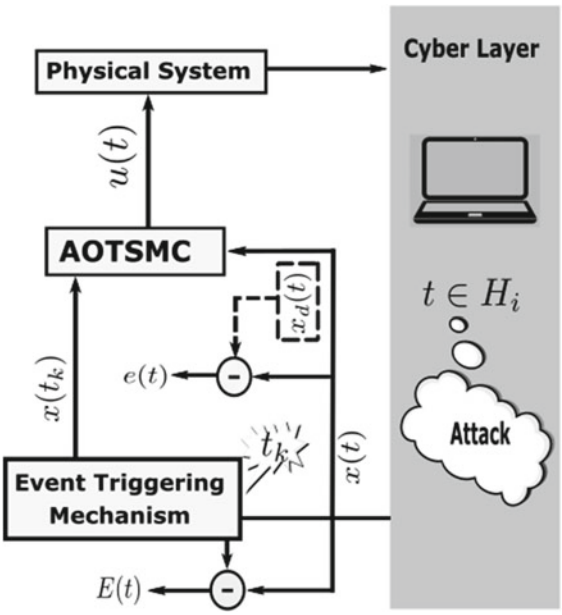

Fig. 2 The schematic representation of the proposed EAOTSMC approach

2.1 Problem Formulation

This section presents an adaptive optimal TSMC (AOTSMC) approach for an uncertain nonlinear dynamic systems. AOTSMC benefits from the fact that there is no reaching phase involved, and it guarantees stability in a fast finite time while fulfilling optimal criteria. Assume the sliding surface is designed as follows

$$S(t) = \vartheta_2 \, \Theta(x, t) + \vartheta_1 \, e(t), \tag{11}$$

where $e(t) = x(t) - x_d(t)$ expresses tracking error, and the known desired states is defined by $x_d(t)$. $\Theta(x, t)$ is an auxiliary state that is defined in the rest of this section, and ϑ_1, ϑ_2 are positive constants.

Assumption 1 Time-dependent derivatives of $x_d(t)$ exist.

Assumption 2 $x_d(t)$, $\dot{x}_d(t)$, $\ddot{x}_d(t) \in \mathcal{L}^\infty$ holds for all $t \in R_{\geq 0}$.

Assumption 3 $f(x(t))$, $\dot{f}(x(t))$ satisfy Lipchitz criterion. Then one can obtain

$$L_0 \left\| x(t_2) - x(t_1) \right\| - \left\| \dot{f}(x(t_2)) - \dot{f}(x(t_1)) \right\| \geq 0, \tag{12}$$

where $L_0 \in R_{>0}$.

Assumption 4 Following inequality holds by $f(x(t))$ for all $t \in R_{\geq 0}$,

$$\bar{\alpha} - \left\| f(x(t)) \right\|_\infty \geq 0, \tag{13}$$

where $\bar{\alpha} \in R_{>0}$.

Assumption 5 A bound is established on the deviation rate of uncertain dynamic and external disturbance inputs as follows,

$$\bar{\beta} \left\| x(t) \right\| - \left\| \dot{\Delta} f(x(t)) + \dot{d}(x, t) \right\| \geq 0, \tag{14}$$

where $\bar{\beta} \in R_{>0}$.

Let's rewrite dynamic equation (10) as:

$$\begin{bmatrix} \dot{x}(t) \\ \dot{x}_{n+1}(t) \end{bmatrix} = \begin{bmatrix} f(x(t)) + \Delta f(x(t)) + d(x, t) \\ 0 \end{bmatrix} + \begin{bmatrix} bu(t) \\ \Psi(t) \end{bmatrix}, \tag{15}$$

where $\Psi(t) = \dot{\Theta}(x, t)$ is an auxiliary input, $x_{n+1}(t) = \Theta(x, t)$ is an auxiliary state, where $\Theta(x, 0) = -\vartheta_1 e(0)/\vartheta_2$.

From (11) time derivatives of sliding surface is defined as:

$$\dot{S}\ (t) = \vartheta_1 \dot{x}(t) - \vartheta_1 \dot{x}_d(t) + \vartheta_2 \dot{\Theta}(x,\ t), \tag{16}$$

and,

$$\ddot{S}(t) = \vartheta_1 \ddot{x}(t) - \vartheta_1 \ddot{x}_d(t) + \vartheta_2 \ddot{\Theta}(x, t). \tag{17}$$

In this study, the terminal manifold is defined as,

$$\delta(t) = \Gamma \dot{S}^{p \times q^{-1}}(t) + S(t), \tag{18}$$

where $\Gamma \in R_{>0}$, and $p,\ q$ are odd constants that satisfy constraint $1 < p \times q^{-1} < 2$.

Theorem 1 *The control input* (19) *guarantees the finite-time global stability of dynamic system* (10) *while the optimal criteria* (20) *is satisfied.*

$$u(t) = \frac{-\vartheta_2}{\vartheta_1 b} \times \Psi(t) + \int_0^t \frac{q}{\vartheta_1 bp} \dot{S}^{1-p\times q^{-1}}(t)(-\dot{S}(t)) - b^{-1} \times (\ddot{x}_d(t) + \dot{f}(x(t)) + (\widehat{\beta}(t) + \beta_0)\text{sgn}(\delta(t))\, \|x(t)\|)dt, \tag{19}$$

and,

$$J = \int_0^\infty \{R\Psi^2(\tau) + (X^T(\tau)Q(X(\tau))X(\tau))\}d\tau, \tag{20}$$

and,

$$\dot{\hat{\beta}}(t) = \{p \times q^{-1}\}\Gamma \dot{S}^{\{p\times q^{-1}-1\}}(t)\vartheta_1 \|\delta(t)\| \|x(t)\|, \tag{21}$$

where $\hat{\beta}(t)$ is an adaptation term, $X(t) = [x(t), \Theta(t)]$ is the auxiliary state vector, Γ, β_0, $R \in R_{>0}$, and $Q(X(t))$ is the positive diagonal matrix. Then, Ψ is expressed as follows,

$$\Psi(t) = R^{-1}B^T \Upsilon X(t), \tag{22}$$

where Υ can be deduced from solving the Riccati equation as follows,

$$A^T(X(t))\Upsilon + \Upsilon A(X(t)) - \Upsilon B R^{-1}(X(t))B^T\Upsilon = -Q(X(t)), \tag{23}$$

where $B = [0_{n\times 1}, 1]^T \in \mathbb{R}^{(n+1)\times 1}$, $A(X(t)) = [\Xi_{n\times n+1}(t), 0_{1\times n+1}] \in \mathbb{R}^{(n+1)\times(n+1)}$. Note that $\Xi_{n\times n}(t)$ can be derived from following equation,

$$\dot{X}(t) = A(X(t))X(t) + B\Psi(t). \tag{24}$$

Due to functionality of the presented approach to deal with the uncertain terms, and converging states in the closed region $\|x(t)\| < r,\ r \in R_{>0}$, in formulation (24), the uncertain term is ignored.

Now, we are in the position to present the event-based controller by providing Theorem 2.

Theorem 2 *Consider an uncertain nonlinear dynamic system (10). Then, control input (25) under event-triggering rule (27) guarantees ultimately global stability of the closed-loop response. Note that under the presented methodology the minimum inter-sampling time, i.e., $\bar{\Delta}$ satisfies inequality (26).*

$$u(t) = -b^{-1}\vartheta_1{}^{-1}\vartheta_2\Psi(t_k) - \int_{t_k}^{t} \vartheta_1{}^{-1}b^{-1}\Gamma^{-1}qp^{-1}\dot{S}^{2-pq^{-1}}(t_k) + b^{-1}(\dot{f}(x(t_k)) - \ddot{x}_d(t) + (\widehat{\beta}\ (t_k) + \beta_0)\,\|x(t_k)\|\,sgn(\delta(t_k)))dt, \tag{25}$$

and,

$$\bar{\Delta} \leq \frac{1}{L_0}\ln\left(\frac{1}{\frac{k_2}{L_0}(\frac{1}{\bar{\lambda}}+1)}+1\right), \tag{26}$$

where $k_2 = \max\{\left\|\vartheta_1{}^{-1}\vartheta_2 R^{-1}B^T\Upsilon\right\|_\infty, 1\}$ for all $t \in [t_k, t_{k+1})$. The event-triggering rule is defined as,

$$\|E(t)\| - \bar{\lambda} \times \{\|X(t)\| + (k_0 + k_1)\} \leq 0, \tag{27}$$

where $\bar{\lambda}$ is a positive constant. Triggering-error is described by $\mathrm{E}(t) = x(t_k) - x(t)$ for all $t \in [t_k, t_{k+1})$, and $k_0 = \|\dot{x}_d(t)\|_\infty + \|\Delta f(x) + d(x,t)\|_\infty, k_1 = \max(|\varphi_2 + \varphi_1|)$ where $\varphi_1 = \int_{t_k}^{t}(\Gamma^{-1}\vartheta_1{}^{-1}\frac{q}{p}\dot{S}^{2-p/q}(t_k)dt$, $\varphi_2 = \int_{t_k}^{t}(\beta_0 + \widehat{\beta}\ (t_k))\,\|x(t_k)\|\,sgn(\delta(t_k)))dt$.

Corollary 1 *Criterion (26) specifies the required minimum inter-sampling-time, and maximum band-width to achieve the closed-loop finite-time stability.*

Proof There are two steps that can be taken to prove the presented theorem. In the first step, it is demonstrated that if (27) holds, then the system dynamic (10) under control input (25) achieves finite-time stability. Then, it is shown that (26) holds under the presented control law and event-triggering rule.

Step 1: We start with the Lyapunov function below

$$V(t) = 0.5 \times \beta_{\Gamma_0}{}^{-1}(\tilde{\beta}^2(t) + \delta^2(t)), \tag{28}$$

where for all $t \in R_{>0}$, $\beta_{\Gamma_0} = \max\{(\tilde{\beta}^2(t) + \delta^2(t))\}$ that guarantees $\|V(t)\| \leq 1$, and $\tilde{\beta}(t) = \widehat{\beta}\ (t) - \bar{\beta}$. Then, one can obtain:

$$\dot{V}(t) = \delta(t)(\dot{S}(t) + \Gamma p \times q^{-1}\ddot{S}(t)\dot{S}^{\{p\times q^{-1}\}-1}(t)) + (\tilde{\beta}(t)\dot{\widehat{\beta}}(t)), \tag{29}$$

where $x_d(t)$ is a known desired signal for all $t \in R_{>0}$. Then, from (29) and (25) one can obtain,

$$\begin{aligned}\dot{V}(t) \leq\ & \beta_{\Gamma_0}{}^{-1}\delta(t)(\left\|\{p\times q^{-1}\Gamma\}\dot{S}^{\{p\times q^{-1}\}-1}(t)\right\|(\vartheta_1(\dot{d}(t) + \dot{\Delta}f(x(t)) + \dot{f}(x(t))\\ & -(\dot{f}(x(t_k)) + (\widehat{\beta}\ (t_k) + \beta_0)\,\|x(t_k)\|\,sgn(\delta(t_k)))\\ & +\vartheta_2(\ddot{\Theta}(t) - \ddot{\Theta}(t_k)) + q\{p\Gamma\vartheta_1\}^{-1}(\dot{S}^{2-p\times q^{-1}}(t) - \dot{S}^{2-p\times q^{-1}}(t_k))) + \beta_{\Gamma_0}{}^{-1}\times\dot{\widehat{\beta}}(t)\tilde{\beta}(t).\end{aligned} \tag{30}$$

By considering Assumption 11, one can obtain,

$$\begin{aligned}\dot{V}(t) \leq {}& \beta_{\Gamma_0}{}^{-1}\delta(t)\left\|\Gamma pq^{-1}\dot{S}^{\{p\times q^{-1}\}-1}(t)\right\|((\vartheta_1 L_0\|E(t)\| + \vartheta_1\bar{\beta}\|x(t)\| \\ & -\vartheta_1(\beta_0 + \widehat{\beta}\ (t_k))\|x(t_k)\| sgn(\delta(t_k)) + \vartheta_2\ \ddot{\Theta}(t) + q\{p\Gamma\}^{-1}\|(\dot{S}^{2-p\times q^{-1}}(t) - \dot{S}^{2-p\times q^{-1}}(t_k))\|) \\ & + \beta_{\Gamma_0}{}^{-1}\dot{\widehat{\beta}}(t)\tilde{\beta}(t).\end{aligned} \tag{31}$$

A new auxiliary variable β_e is defined as follows,

$$\beta_e = \vartheta_1 L_0\|E(t)\|, \tag{32}$$

where λ, ϑ_1 are chosen small values such that $(\bar{\beta} + \beta_0)\|\delta(t)\|\|x(t_k)\| \gg \beta_e$. Note that according to (21) one can obtain $\hat{\beta}(t) > \beta(t_k), \tilde{\beta}(t) < 0$ for all $t \in [t_k, t_{k+1})$, then,

$$\begin{aligned}\dot{V}(t) \leq {}& \underbrace{-\beta_{\Gamma_0}{}^{-1}\left\|\{p\times q^{-1}\Gamma\}\dot{S}^{\{p\times q^{-1}\}-1}(t)\right\|(-\beta_e + (\beta_0+\bar{\beta})\|x(t_k)\|}_{\mathbb{Z}_0} \\ & \underbrace{+\left|\tilde{\beta}(t)\right|\|x(t)\| - q\times\{p\Gamma\}^{-1}\|(\dot{S}^{2-\{p\times q^{-1}\}}(t) - \dot{S}^{2-\{p\times q^{-1}\}}(t_k))\| - \|\ddot{\Theta}(t)\|\vartheta_2)}_{\mathbb{Z}_0}\|\delta(t)\| \\ & \underbrace{-\beta_{\Gamma_0}{}^{-1}\left\|q^{-1}p\Gamma\dot{S}^{\{p\times q^{-1}\}-1}(t)\right\|\|x(t_k)\|\|\delta(t)\|}_{\mathbb{Z}_1}\left\|\tilde{\beta}(t)\right\|),\end{aligned} \tag{33}$$

then,

$$\dot{V(t)} \leq -\beta_\Gamma V^{0.5}(t), \tag{34}$$

where $\beta_\Gamma = \min\left\{\sqrt{2}\mathbb{Z}_0, \sqrt{2}\mathbb{Z}_1\right\}$.

Step 2: The closed-loop dynamic system under the proposed triggering rule and control effort for all $t \in [t_k, t_{k+1})$ can be expressed as follows,

$$\begin{aligned}\dot{x}(t) = {}& \Delta f(x) + d(x,t) + f(x(t)) + b(-\vartheta_2\vartheta_1{}^{-1}b^{-1}\Psi(t_k) \\ & + \int_0^t[-\Gamma^{-1}\vartheta_1{}^{-1}b^{-1}\frac{q}{p}\dot{S}^{2-p/q}(t_k) \\ & - b^{-1}(\dot{f}(x(t_k)) - \ddot{x}_d(t) + (\widehat{\beta}\ (t_k) + \beta_0)\|x(t_k)\| sgn(\delta(t_k)))]dt,\end{aligned} \tag{35}$$

where $\{x(t_k)|k \in N_0\}$ represents the transmitted data at time-instances t_k in which triggering-rule is satisfied.

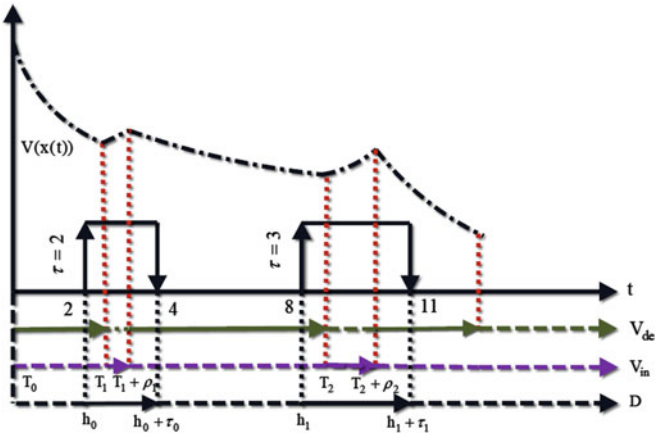

Fig. 3 Typical evolution of Lyapunov function under cyber attack, and event-triggering activation. In this example, $n(1, 9) = 2, n(1, 3) = 1, n(2.5, 9) = 1$ and $D(8, 12) = 3, h = \{2, 8\}$, $D(1, 3) = 1$, and $H_1 = [2, 4)$

$$\begin{aligned}\dot{x}(t) = \Delta f(x) + d(x,t) + f(x(t)) + b(-\vartheta_2 {\vartheta_1}^{-1} b^{-1} \Psi(t_k) \\ + \int_0^t -\Gamma^{-1} {\vartheta_1}^{-1} b^{-1} q\, p^{-1} \dot{S}^{2-\{p\times q^{-1}\}}(t_k) - b^{-1}(\dot{f}(x(t_k))) \\ -\ddot{x}_d(t) + (\beta_0 + \widehat{\beta})\, \|x(t_k)\|\, sgn(\delta(t_k)))dt.\end{aligned} \tag{36}$$

From (36) and (27), we have,

$$\begin{aligned}\dot{\mathrm{E}}(t) = \Delta f(x) + d(x,t) + f(x(t)) - f(x(t_k)) + \dot{x}_d(t) - {\vartheta_1}^{-1}\vartheta_2 \Psi(t_k) \\ - \int_{t_k}^t \Gamma^{-1} {\vartheta_1}^{-1} \frac{q}{p} \dot{S}^{2-p/q}(t_k)dt - \int_{t_k}^t (\widehat{\beta}\ (t_k) + \beta_0)\, \|x(t_k)\|\, sgn(\delta(t_k)))dt,\end{aligned} \tag{37}$$

Considering $\varphi_1 = \int_{t_k}^t (\Gamma^{-1} {\vartheta_1}^{-1} \frac{q}{p} \dot{S}^{2-p/q}(t_k)dt$, $\varphi_2 = \int_{t_k}^t (\widehat{\beta}\ (t_k) + \beta_0)\, \|x(t_k)\|$ $sgn(\delta(t_k)))dt$, and $k_1 = \max(|\varphi_2 + \varphi_1|)$ yield,

$$\dot{\mathrm{E}}(t) \leq L_0\, \|E(t)\| - {\vartheta_1}^{-1}\vartheta_2 \Psi(t_k) + k_0 + k_1, \tag{38}$$

then,

$$\|E(t)\| \leq {L_0}^{-1}(\left\|\vartheta_2 {\vartheta_1}^{-1} R^{-1} B^T \Upsilon\right\|_\infty \|X(t_k)\|_\infty + k_0 + k_1) \times \int_{t_k}^t e^{L_0(t-\tau)} d\tau. \tag{39}$$

Now, with considering $\Im(t) = [E(t), 0]$, $k_2 = \max\{1, \left\|{\vartheta_1}^{-1}\vartheta_2 R^{-1} B^T \Upsilon\right\|_\infty\}$, and $X(t_k) = \Im(t) + X(t)$, Eq. (39) can be represented as,

$$\|\Im(t)\| \leq {L_0}^{-1} k_2(\|\Im(t)\| + \|X(t)\| + k_0 + k_1)(e^{L_0 \bar{\Delta}} - 1), \tag{40}$$

In regards to $\bar{\Delta}$, (40) is monotonically increasing. By taking the stability of $X(t)$ into account, and considering $\|E(t)\| = \|\Im(t)\|$, one can obtain,

$$\bar{\Delta} \leq {L_0}^{-1} \ln(\{\frac{k_2}{L_0}(\frac{1}{\bar{\lambda}} + 1)\}^{-1} + 1). \tag{41}$$

This completes the proof.

2.2 Denial-of-Service Attacks

Section 2.1 presents the stability analysis of the proposed event-based terminal SMC approach. In this section, the effect of the DoS cyber attack on the closed-loop stability is expressed, and the explicit relation between the malicious attack properties, i.e., cyber-attacks duration and frequency, with the closed-loop stability is derived.

To interpret cyber attacks' frequency and duration, the following two assumptions regarding the parameters of the DoS attack are taken into consideration without compromising generality [51].

Assumption 6 The following conditions are true for every $\tau, t \in R_{>0}$:

$$n(\tau, t) \leq n_0 + \frac{t - \tau}{\tau_D}, \tag{42}$$

where $\tau_D, n_0 \in R_{>0}$.

Assumption 7 The following conditions are true for every $\tau, t \in R_{>0}$:

$$D(\tau, t) \leq d_0 + \frac{t - \tau}{T}, \tag{43}$$

where $T, d_0 \in R_{>0}$.

In order to clarify the DoS attacks time period, H_n is expressed as,

$$H_n := [h_n \; h_n + \tau_n[\bigcup_{n \in N_0} \{h_n\}, \tag{44}$$

In the DoS attacks occurrence curve, as depicted in Fig. 3, h_n, $n \in N_0$ represents attack initiation instances, and τ_n represents DoS attacks duration, By considering (43), and (44) one can conclude,

$$D(\tau, t) = \bigcup_{n \in N_0} \{[\tau, t[\bigcap H_n\}. \tag{45}$$

Having made that distinction, we also need to find two time-based clusters different viewpoints. The first cluster illustrates the time duration in which a DoS attack occurs, the second group illustrates the time duration in which (27) is violated.

$$A[\tau, t) = [\tau, t) \backslash D[\tau, t), \tag{46}$$

Using $A(\tau, t)$ and $D(\tau, t)$, the time axis is divided into separate clusters, in which DoS attack occurs and in which it does not. In order to clarify the second group, it is necessary to define two sets V_{in} and V_{de}. These sets are used to show the time instances at which (27) does not hold due to a DoS attack and the time stamps at which (27) remains valid.

$$V_{in} = \bigcup_{i \in N_0} [T_i, T_i + \rho_i)\,, \tag{47}$$

and,

$$V_{de} = \bigcup_{i \in N_0} \left[T_i + \rho_i, T_{i+1}\right). \tag{48}$$

In order to determine whether (27) holds true or not in the domain $[t_1, t_2)$, the following sets are defined, respectively,

$$\bar{A}(t_1, t_2) = V_{dec} \bigcap [t_1, t_2), \tag{49}$$

and,

$$\bar{D}(t_1, t_2) = V_{in} \bigcap [t_1, t_2), \tag{50}$$

Assumption 8 It is assumed that no attack occurs at the beginning of communication, thus $T_0 = \rho_0 = 0$.

Figure 3 describes the groups and sets that are proposed. It is now critical to deriving constraints on the parameters of the DoS attack with respect to their impact on V_{in} and V_{de}, as will be discussed in the following subsection.

2.3 Stability and Cyber Attacks

As mentioned in the previous subsections, satisfying (26), and (27) guarantee the closed-loop stability. It is now possible to investigate the situation in which (26), (27) are not valid due to malicious attacks. The solution of (34) is expressed by

$$V(t) \leq V(0)\, e^{-\beta_\Gamma t}. \tag{51}$$

Now from (33) we have,

$$\begin{aligned}\dot{V}(t) \leq & -\underbrace{\beta_{\Gamma_0}{}^{-1}\left\|pq^{-1}\Gamma\dot{S}^{\{p\times q^{-1}\}-1}(t)\right\|}_{\chi_3}[((\bar{\beta}+\beta_0)\|x(t_k)\|-\vartheta_2\|\ddot{\Theta}(t)\|) \\ & \underbrace{+\left|\tilde{\beta}(t)\right|\|x(t)\|-\{p\Gamma\}^{-1}\times q\|(\dot{S}^{2-p\times q^{-1}}(t)-\dot{S}^{2-p\times q^{-1}}(t_k))\|]}_{\chi_3}\|\delta(t)\| \\ & -\underbrace{\beta_{\Gamma_0}{}^{-1}\left\|p\Gamma\times q^{-1}\dot{S}^{p/q-1}\right\|\|\delta(t)\|\|x(t_k)\|}_{\chi_4}\left\|\tilde{\beta}(t)\right\| \\ & +\beta_{\Gamma_0}{}^{-1}\vartheta_1 L_0\left\|p\Gamma q^{-1}\dot{S}^{\{p\times q^{-1}\}-1}\right\|\|E(t)\|\|\delta(t)\|,\end{aligned} \tag{52}$$

with defining $\beta_{\Gamma_2}=\min\left\{\sqrt{2}\chi_3,\sqrt{2}\chi_4\right\}$, $\beta_{\Gamma 3}=\max(\frac{\vartheta_1 L_0}{\beta_{\Gamma_0}}\left\|\Gamma\frac{p}{q}\dot{S}^{p/q-1}\right\|\|\delta(t)\|)$, and considering $\|V(t)\|\leq 1$ one can obtain,

$$\dot{V}(t)\leq\beta_{\Gamma 3}\|E(t)\|-\beta_{\Gamma_2}V(t). \tag{53}$$

The solution of (53) can be restated as,

$$V(t)\leq\beta_{\Gamma 3}\times\beta_{\Gamma_2}{}^{-1}\|E(t)\|+exp\{-\beta_{\Gamma_2}t\}V(0), \tag{54}$$

By having (27), (51) can be expressed for all $t\in V_{de}$ as,

$$V(t)\leq V(T_i+\rho_i)exp\{-\beta_\Gamma(t-T_i-\rho_i)\}, \tag{55}$$

while (27) does not hold, for all $t\in V_{in}$, (51) results

$$V(t)\leq exp\{-\beta_{\Gamma_2}(t-T_i)\}V(T_i)+\beta_{\Gamma 3}\beta_{\Gamma_2}{}^{-1}\|E(t)\|, \tag{56}$$

By considering Assumptions 6, and 7 one can obtain,

$$\begin{aligned}&V(t)\leq exp\{-\beta_\Gamma\left|\bar{A}(0,t)\right|-\beta_{\Gamma_2}\left|\bar{D}(0,t)\right|\} \\ &+\beta_{\Gamma 3}\times\beta_{\Gamma_2}{}^{-1}\|E(t)\|\ (1+\sum_{i\in N_2 t>T_i}(exp\{-\beta_\Gamma\left|\bar{A}(T_i,t)\right|-\beta_{\Gamma_2}\left|\bar{D}(T_i,t)\right|\})),\end{aligned} \tag{57}$$

then,

$$\begin{aligned}\|E(\tau,t)\|_{\max}<&(\alpha+k_0)(n_0+\tfrac{t-T_i}{\tau_D})(d_0+\tfrac{t-T_i}{T}) \\ &+(1+n)\bar{\Delta}\leq e^{(\alpha+k_0)(n_0+\frac{t-T_i}{\tau_D})(d_0+\frac{t-T_i}{T})+(1+n)\bar{\Delta}}.\end{aligned} \tag{58}$$

Considering (49), and (50) yield,

$$-\beta_\Gamma\left|\bar{A}(T_i,t)\right|-\beta_{\Gamma_2}\left|\bar{D}(T_i,t)\right|=(\beta_\Gamma-\beta_{\Gamma_2})\bar{D}(T_i,t)-\beta_\Gamma(t-T_i). \tag{59}$$

The upper bound of right-hand-side of (57) should be specified, then

$$1+\sum_{\substack{i\in N_2\\ t>T_i}} exp\{-\beta_\Gamma\left|\bar{A}(T_i,t)\right|-\beta_{\Gamma_2}\left|\bar{D}(T_i,t)\right|\}\leq 1+\sum_{\substack{i\in N_2\\ t>T_i}} e^{\varpi}, \tag{60}$$

where,

$$\varpi=(\beta_\Gamma-\beta_{\Gamma_2})\bar{D}(T_i,t)+(\alpha+\upsilon)(n)\bar{D}(T_i,t)+((1+n)(\alpha+\upsilon)-\beta_\Gamma)\bar{\Delta}. \tag{61}$$

The stability is guaranteed if $\varpi<0$, then

$$(\beta_\Gamma-\beta_{\Gamma_2})\bar{D}(T_i,t)+(\alpha+\upsilon)(n)\bar{D}(T_i,t)< \quad(\beta_\Gamma-(\alpha+\upsilon)(1+n))\bar{\Delta}, \tag{62}$$

finally,

$$\bar{D}(T_i,t)<\frac{(\beta_\Gamma-(\alpha+\upsilon)(1+n))}{(\beta_\Gamma-\beta_{\Gamma_2})+(n)(\alpha+\upsilon)}\bar{\Delta}. \tag{63}$$

2.4 Results and Discussion

The presented resilient AOFTSMC is validated in this section. To achieve this goal, a numerical example is provided as follows. Consider an uncertain nonlinear dynamic system as,

$$\begin{aligned}\dot{x}_1(t)&=x_2(t)\\ \dot{x}_2(t)&=-x_1^2(t)+x_2(t)+\Delta f(x(t))+d(x,t)+u(t).\end{aligned} \tag{64}$$

where $x_1(t)$, $x_2(t)$ are system states, $u(t)$ expresses the control input, unknown system dynamic is defined by $\Delta f(x(t))=0.1x_1(t)$, and $d(x,t)=\sin(t)$ represents the disturbance applied to the system. From (33), and (52) one can obtain that $\beta_\Gamma\approx\beta_{\Gamma_2}$ if β_0, ϑ_2 are chosen appropriate values. Then, inequality (63) can be simplified as,

$$\bar{D}(T_i,t)<\lambda_4\bar{\Delta}, \tag{65}$$

where $\lambda_4=\frac{(\beta_\Gamma-(1+n)(\alpha+\upsilon))}{(\alpha+\upsilon)(n)}$. Consider $\vartheta_1=1$, $\beta_0=10$, $\vartheta_2=0.1$, $\bar{\lambda}=0.0001$, $q=5$, $p=3$, $\alpha=2$, $k_2=1$ and $L_0=2$. Then, minimum inter-sampling time $\bar{\Delta}=9.8\times10^{-5}$ is derived through (41). Since (41) decreases as k_2 increases, the worst-case scenario for k_2 is considered during simulation. As illustrated in Fig. 5, none of the inter-sampling duration is less than 0.0001, which verifies the proposed criterion (41). In order to calculate the maximum length of an endurable malicious attack, it would be reasonable to assume that $t-\tau=1$/s and $n=1$. It is obvious that increasing n results in decreasing the affordable duration of time that a given attack can last.

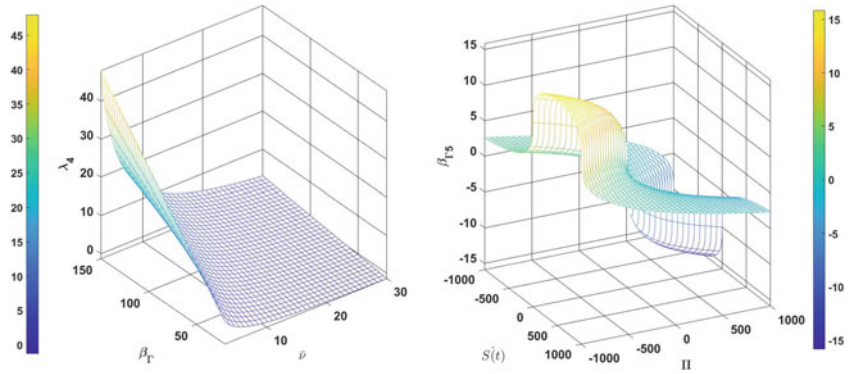

Fig. 4 Left: A numerical analyses of λ_4 and the effect of β_Γ and $\bar{\upsilon} = \alpha + \upsilon$ variations on a tolerable DoS attack's duration are presented. Right: Numerical variations of $\beta_{\Gamma_5} = \dot{S}^{2-p\times q^{-1}}(t) - \dot{S}^{2-p\times q^{-1}}(t_k)$, $\Pi = \dot{S}(t) - \dot{S}(t_k)$ due to the DoS attacks is depicted

Table 1 Variance and mean values of states under cyber-attack

states	DoS attack duration per second (%)	Γ	[Mean/Variance]
$[x_1(t), x_2(t)]$	5	10	[0.014/0.11, −0.01/0.04]
$[x_1(t), x_2(t)]$	10	100	[0.02/0.01, −0.01/0.05]

Figure 5 shows that when states converge to zero, the sampling rate is decreased. Note that when states are stabilized, the inter-sampling time is increased since the event-triggering mechanism is not activated. Figure 6 shows the response of the auxiliary state $x_3(t)$ as well as the augmented input Ψ. Contrary to some studies such as [3, 40, 52] where the focus is on linear dynamic systems, the proposed formulation concerns with the standard nonlinear systems. Also, by specifying the least possible inter-sampling time, it provides the maximum required network bandwidth.

The effect of β_Γ and $\bar{\upsilon} = \upsilon + \alpha$ variations is shown in Fig. 4. Increasing the value of β_Γ results in an increasing convergence rate that increases the endurable cyber-attacks' duration. Meanwhile, the tolerability under malicious DoS attacks during V_{in} is improved while $\bar{\upsilon}$ decreases.

Simulation results are presented in Table 1 under various DoS attack duration with different values of Γ and β_Γ. As shown in this table, the stability is preserved under various conditions.

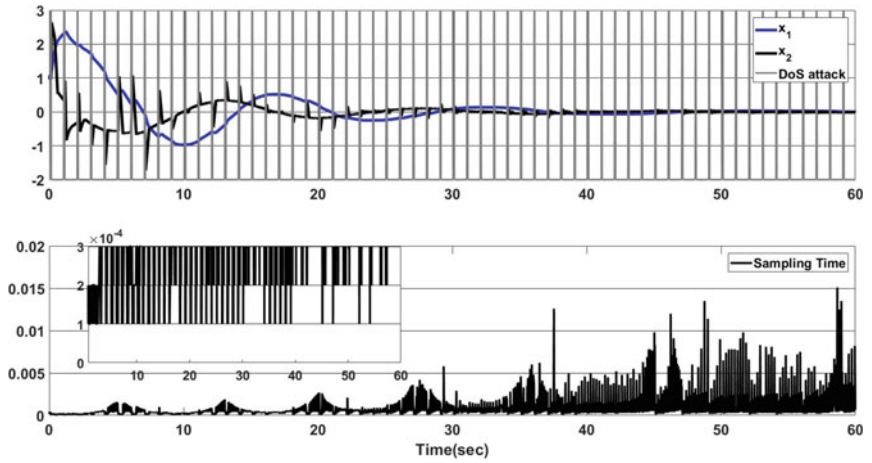

Fig. 5 Simulation results of system in (64) using the control effort (25) and under the cyber attacks. Top: System responses in closed-loop with $x(0) = [1\ ,\ 1]$. Bottom: inter-sampling times that are produced using the proposed event-triggering method

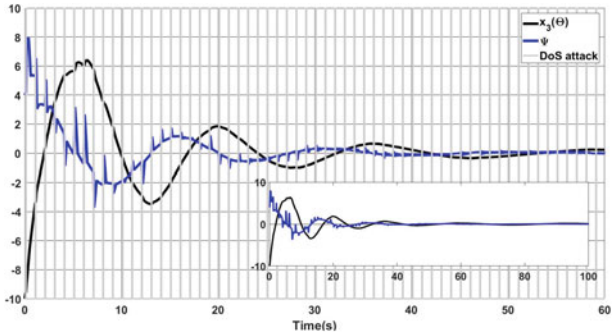

Fig. 6 Evolution of $\Psi(t)$ and $x_3(t)$ using the control effort in (25) and under the malicious cyber-attacks

3 Quantized Event-Triggered Terminal SMC Design for Uncertain Input-Delayed Dynamic

As outlined in Sects. 1 and 2, an overview of event-based approaches, their challenges, and their effects are described in detail. This section examines the effects of quantizers in closed-loop systems with event-based terminal SMC. There is a strong relationship between an event-triggering rule and quantized signal during the development of CPSs, from both a theoretical as well as a practical perspective. Keeping control precision and stability is one of the most significant objectives when a physical system is communicating digitally, with certain considerations and constraints. For instance, the maximum number of bits that can be transmitted through a data-packet over a

network layer [22], quantization error [23], and sensitivity adjustment in dynamic quantizers are all critical considerations and limitations that must be considered.

This paper presents a novel design approach for dynamic quantizers that considers event-tagging rules for uncertain input-delayed nonlinear dynamic systems. In contrast, most studies centered on the development of quantization methodologies for certain linear dynamics [24, 26] or they focused on determining the continuous-time evolving of quantizer parameters.

3.1 Problem Formulation

Consider an uncertain input-delayed nonlinear system as follows,

$$\dot{x}(t) = f(x(t)) + \Delta f(x(t)) + bu(t - D) + d(x, t), \tag{66}$$

where $x(t) = [x_1(t), \ldots, x_n(t)] \in \mathbb{R}^n$ is the state vector with initial condition $x(0) = x_0$, uncertain dynamics are defined by $\Delta f(x(t)) \in \mathbb{R}^n$, and $d(x, t) \in \mathbb{R}$ shows bounded external disturbance that satisfies $\|d(x, t)\| \leq \bar{d}$, where $\bar{d} \in R_{>0}$. A control input signal is shown by $u(t) \in \mathbb{R}^n$, $b \in R_0$ is a constant parameter, and $D \in R_0$ is the known input delay.

Assumption 9 The dynamic system (66) does not show any finite escape time behavior $t \in [0, D)$ [53].

Assumption 10 $x_d(t)$, $\dot{x}_d(t)$, $\ddot{x}_d(t) \in \mathcal{L}^\infty$ holds for all $t \in R_{\geq 0}$.

Assumption 11 $f(x(t))$, $\dot{f}(x(t))$ satisfy Lipchitz criterion as follows,

$$\left\| \dot{f}(x(t_2)) - \dot{f}(x(t_1)) \right\| \leq L_0 \left\| x(t_2) - x(t_1) \right\|, \tag{67}$$

where $L_0 \in R_{>0}$.

Assumption 12 Following inequality holds by $f(x(t))$ for all $t \in R_{\geq 0}$,

$$\bar{\alpha} - \|f(x(t))\|_\infty \geq 0, \tag{68}$$

where $\bar{\alpha} \in R_{>0}$.

Assumption 13 A bound is established on the deviation rate of uncertain dynamic and external disturbance inputs as follows, $\Delta f(x(t))$ and $d(x, t)$ satisfy the following condition in $t \in R_{\geq 0}$,

$$\bar{\beta} \|x(t)\| - \left\| \dot{\Delta} f(x(t)) + \dot{d}(x, t) \right\| \geq 0, \tag{69}$$

where $\bar{\beta} \in R_{>0}$.

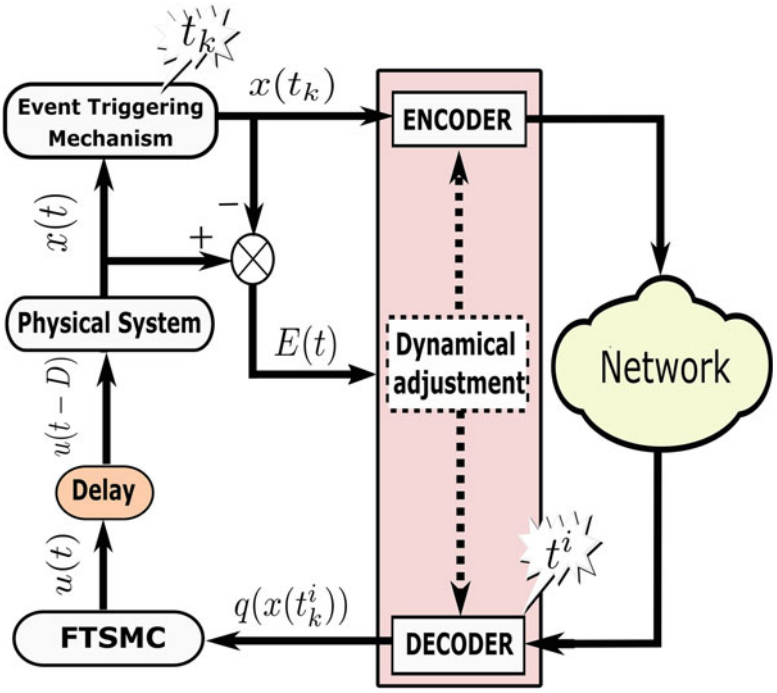

Fig. 7 Block diagram representation of the proposed scheme

It is essential for the design procedure methodology to be guided by the presented assumptions. Lipchitz's criteria are generally satisfied by most physical systems. In the meantime, engineers possess the knowledge of the boundaries of uncertainty terms and disturbances through their practical experience. Then, the proposed assumptions are not restrictive.

It is the purpose of the present section to demonstrate robust scheme for uncertain systems, which use the network layer to convey measurement data despite input delays and quantizers. Accordingly, this study adopts a quantized event-trigger SMC. Figure 7 illustrates the block diagram of the proposed scheme.

According to Fig. 7, the event-trigger mechanism updates the measured states in the time stamps according to the predefined rules that are outlined in the remainder of this section. After being quantized by a dynamic quantizer, measurement data are transmitted through the network layer as part of the digital communication layer. Quantization involves mapping time-varying continuous time signals into piecewise constant signals. The dynamic quantizer described in this study is as follows [24, 54],

$$q_\tau(z(t)) = \tau q(z(t)\tau^{-1}), \tag{70}$$

where $\tau \in R_{>0}$ is adjusted in each quantization time stamp, $z(t)$ is a continues- time signal, and $q(.)$ is defined as follows,

$$\|q(z(t)) - z(t)\| < \mu\,,\ if \quad \|z(t)\| < M, \tag{71a}$$

$$\|q(z(t))\| > M - \mu,\ if \quad \|z(t)\| > M, \tag{71b}$$

where $M \in R_{>0}$ is the quantizer saturation level, and $\mu \in R_{>0}$ is quantization error bound parameter. Vector quantization consists of dynamic quantization of each component of the vector, i.e. $q_\tau(Z(t)) = [q_\tau(z_1(t)), q_\tau(z_2(t)), \ldots, q_\tau(z_n(t))]$ where $Z(t) \in \mathbb{R}^{1\times n}$, and a piece-wise constant signal will be created for each component with a value in the set as $\mathbb{N} = \{-\lceil M\rceil\,\tau(t),\ (-\lceil M\rceil + 1)\tau(t), \ldots, (\lceil M\rceil + 1)\tau(t),\ \lceil M\rceil\,\tau(t)\}$. $x(t_k)$ is produced by the event-triggering rule, and passed through an encoder, then transmitted through the network layer. Then measurement data are decoded at time stamps $t^i, i \in N_0$. Finally, the designed FTSMC controller uses $x(t_k^i)$ to produce a control effort signal. $x(t_k^i)$ is defined as:

$$x(t_k^i) = q_{\mu^i(t)}(x(t)), \tag{72}$$

where $t \in \{(t_k, t_{k+1}) \bigcap (t^i, t^{i+1})\}$ and $t_k, k \in N_0$ are triggering time instances. Then, t_{k+1} is expressed as follows.

$$t_{k+1} = \inf\{t \in (t_k, \infty),\ k \in N\}. \tag{73}$$

Note that $t^i, i \in N_0$ start counting in the duration of $[t_k, t_{k+1})$, i.e. $t_0 < t^0 < t^1 < \cdots < t_1 < t^0 < t^1 < \cdots < t_2, \ldots$ According to (70) and (71), $e_k^i(t)$ in the time domain $t \in \{(t_k, t_{k+1}) \bigcap (t^i, t^{i+1})\}$ is expressed as,

$$e_k^i(t) = x(t_k^i) - x(t_k) \tag{74}$$

From (71) and (74), one can obtain,

$$\left\|e_k^i(t)\right\| \le \mu_{t^i}\,,\ if \quad \|x(t_k)\| < M, \tag{75a}$$

$$\left\|e_k^i(t)\right\| > M - \mu_{t^i},\ if \quad \|x(t_k)\| > M. \tag{75b}$$

The main conclusion that can be drawn from this subsection is that states are sampled at time instances $t_k, k \in N_0$, and when relaxation time arrives, i.e. $[t_k, t_{k+1})$, states' quantization time instances are represented by stamp t^i, $i \in N_0$. The next subsection presents the controller design approach.

3.2 Control Methodology

The aim of this section is to develop an adaptive fast terminal SMC controller that guarantees finite-time convergence stability is proposed.

Theorem 3 *Consider a dynamic system* (66) *while* $D = 0$. *A control signal (76) grantees the finite-time asymptotically stability.*

$$u(t) = -\int_0^t [q\,p^{-1}{\alpha_1}^{-1} b^{-1} \dot{S}^{2-p/q}(t) + b^{-1}(-\ddot{x}_d(t) + \dot{f}(x(t)) + (\widehat{\beta}\ (t) + \\ + \beta_0)\,\|x(t)\|\,\mathrm{sgn}(\delta(t)))]dt, \tag{76}$$

where $S(t)$ is the sliding surface and is considered as,

$$S(t) = \alpha_1 e(t), \tag{77}$$

where $\alpha_1 \in R_{>0}$. $\delta(t)$ is the terminal manifold and is represented as,

$$\delta(t) = k_2 S(t) + k_1 \dot{S}^{p\times q^{-1}}(t), \tag{78}$$

where $k_1 \in R_{>0}$. Tracking error is expressed by $e(t) = x(t) - x_d(t)$, and p, q are two odd numbers that satisfy $1 < \frac{p}{q} < 2$. Finally, adaptation law is defined as follows,

$$\dot{\widehat{\beta}}(t) = k_1 pq^{-1} \dot{S}^{\{p\times q^{-1}\}-1}(t)\,\|x(t)\|\,\|\delta(t)\|\,\alpha_1, \tag{79}$$

where $\widehat{\beta}\ (0) = \beta_0$ is the initial condition and satisfies $\beta_0 \geq \bar{\beta}/2$.

Proof of Theorem 3. A Lyapunov function candidate is chosen as:

$$V(t) = 0.5\{\,\delta(t)^T \delta(t) + \tilde{\beta}^T \tilde{\beta}(t)\}, \tag{80}$$

where adaptation error is considered as $\tilde{\beta}(t) = \widehat{\beta}\ (t) - \bar{\beta}$. From (80), (78) one can obtain,

$$\dot{V}(t) = \delta(t)^T \big[\dot{S}(t) + k_1\alpha_1 pq^{-1}\dot{S}^{\{p\times q^{-1}-1\}}(t)\times \\ \big\{\dot{f}(x(t)) + \Delta\dot{f}(x(t)) + \dot{d}(x,t) + b\dot{u}(t) - \dddot{x}_d\big\}\big] + \tilde{\beta}(t)^T \dot{\widehat{\beta}}(t). \tag{81}$$

Substitution $u(t)$ from (76) yields,

$$\dot{V}(t) = \delta(t)\Big[k_1\alpha_1 p \times q^{-1}\dot{S}^{\{p\times q^{-1}-1\}}(t)\times \Big\{\Delta\dot{f}(x(t)) + \dot{d}(x,t) - (\widehat{\beta}\ (t) + \beta_0)\,\|x(t)\|\, sgn(\delta(t))\Big\}\Big] + \tilde{\beta}(t)\dot{\widehat{\beta}}(t). \tag{82}$$

From Assumption 13 and (79) one can obtain,

$$\dot{V}(t) \le k_1\alpha_1\frac{p}{q}\dot{S}^{p/q-1}(t)\,\|\delta(t)\|\,\{\bar{\beta}\,\|x(t)\| - (\widehat{\beta}\ (t) + \beta_0)\,\|x(t)\| + (\widehat{\beta}\ (t) - \bar{\beta})\,\|x(t)\| + \left\|\tilde{\beta}(t)\right\|\|x(t)\| - \left\|\tilde{\beta}(t)\right\|\|x(t)\|\}. \tag{83}$$

Then,

$$\dot{V}(t) \le -\underbrace{\Big\{k_1\alpha_1 pq^{-1}\dot{S}^{p\times q^{-1}-1}(t)(\beta_0 - \left\|\tilde{\beta}(t)\right\|)\,\|x(t)\|\Big\}}_{\xi_1}\|\delta(t)\| - \underbrace{\{k_1\alpha_1 p\times q^{-1}\dot{S}^{p/q-1}(t)\,\|x(t)\|\}}_{\xi_2}\left\|\tilde{\beta}(t)\right\|, \tag{84}$$

then,

$$\begin{aligned}\dot{V}(t) &\le -\min\{\sqrt{2}\xi_1, \sqrt{2}\xi_2\}\frac{1}{\sqrt{2}}\left[\left\|\tilde{\beta}\right\| + \|\delta(t)\|\right]\\ &\le -\min\{\sqrt{2}\xi_1, \sqrt{2}\xi_2\}V(t)^{1/2}.\end{aligned} \tag{85}$$

3.3 *Quantized Event-Triggered Control Design*

Compared to the time-triggered mechanism, the event-based approach reduces computation load and provide resilient behavior while data-packets are lost through the network layer. As stated in the introduction section, measurement data are updated when triggering criteria is satisfied at time stamps t_k. Consider event-triggering error as follows,

$$E(t) - x(t) + x(t_k) = 0, \tag{86}$$

where $E(t_k) = 0$ for all $k \in N_0$. The quantized event-based fast terminal SMC is designed for an uncertain input-delayed nonlinear dynamic (66) in this subsection. Consider the sliding surface in the following manner,

$$S(t) = \alpha_1 e(t) + \alpha_2\Theta(t), \tag{87}$$

where $\alpha_2 = b\alpha_1$, $\alpha_1 \in R_{>0}$, where $\Theta(t) = \int_{t-D}^{t} u(\tau)\, d\tau$. Note that initial condition of $\Theta(t)$ is zero, and the terminal sliding manifold is defined according to (78).

Lemma 1 *The area Ω in which $sgn(S(x(t_k^i))) \neq sgn(S(x(t_k)))$ is the infinitesimally closed region.*

Proof Consider the quantizer that is defined by (70) and (71), where one can obtain $sgn(x(t_k^i)) = sgn(x(t_k))$. Consider (86), (90), and suppose that the last successful transmitted measurement data is $x(t_k)$. Now, suppose that $x(t)$, $t \in [t_k, t_{k+1})$ tends toward zero, then, consider t^* represents time instance in which $x(t^*) = 0$, then,

$$\lim_{x(t)\to 0} \|E(t)\| = 0. \tag{88}$$

$\|x(t)\| > 0$ for $t^* < t$ and according to (90), triggering rule is then activated, and $sgn(x(t_k) = sgn(x(t))$. As a result, considering (87) yields $sgn(S(x(t_k^i))) = sgn(S(x(t)))$ in $t \in [t_k, t_{k+1})$.

This completes the proof.

Theorem 4 *Consider the dynamic system (66) under triggering-rule (90), and dynamic quantizer (72). Then, the control effort (89) guarantees globally uniformly ultimately bounded (GUUB) stability.*

$$\begin{aligned} u(t) = -\int_{t^i}^{t} & k_1{}^{-1}\alpha_1{}^{-1}b^{-1}k_2\frac{q}{p}\dot{S}^{2-p/q}(t_i^k) + b^{-1}(\dot{f}(x(t_k^i)) \\ & - \ddot{x}_d(t) + (\bar{\beta} + \beta_0)\left\|x(t_k^i)\right\| \operatorname{sgn}(\delta(t_k^i)))dt. \end{aligned} \tag{89}$$

Note that $u(t) = 0$ for $t \in [0, D)$. Triggering- rule is defined as,

$$\|E(t)\| - \lambda \|x(t)\| \leq 0, \tag{90}$$

for $t \in \{(t_k, t_{k+1}) \bigcap (t^i, t^{i+1}) | i, k \in N_0\}$, $\delta(t_k^i) = q_{\mu^i(t)}(\delta(x(t_k)))$, $\dot{S}(t_k^i) = q_{\mu^i(t)}(\dot{S}(x(t_k)))$, $\bar{\beta} \in R_{>0}$.

Proof of Theorem 4. Lyapunov function candidate is expressed as,

$$V(t) = 0.5\delta(t)^T\, \delta(t). \tag{91}$$

The first time derivation of sliding surface yields,

$$\dot{S}(t) = \alpha_1\dot{x}(t) - \alpha_1\dot{x}_d(t) + \alpha_2\dot{\Theta}(x, t), \tag{92}$$

then,

$$\ddot{S}(t) = \alpha_1(\dot{f}(x(t)) + \Delta\dot{f}(x(t)) + \dot{d}(x, t) + b\dot{u}(t - D)) - \alpha_1\ddot{x}_d(t) + \alpha_2(\dot{u}(t) - \dot{u}(t - D)). \tag{93}$$

From (91), and (78) we have,

$$\dot{V}(t) = \delta(t)^T (k_2 \dot{S}(t) + k_1 \frac{p}{q} \ddot{S}(t) \dot{S}^{p/q-1}(t)). \tag{94}$$

Taking (93), and (94) into consideration yields,

$$\begin{aligned} \dot{V}(t) = \delta(t)^T \{p \times q^{-1}\} k_1 \dot{S}^{\{p\times q^{-1}\}-1}(t) \\ \times \left\{ q \times \{pk_1\}^{-1} k_2 \dot{S}^{2-p\times q^{-1}}(t) + b\alpha_1 \dot{u}(t) + \alpha_1 \Gamma \right\}, \end{aligned} \tag{95}$$

where $\Gamma = \left[\dot{f}(x(t)) + \dot{\Delta} f(x(t)) + \dot{d}(t) - \ddot{x}_d(t) \right]$. From (89) and (95) one can conclude,

$$\begin{aligned} \dot{V}(t) \leq \delta(t)^T \alpha_1 k_1 p q^{-1} \dot{S}^{\{p\times q^{-1}-1\}}(t) \{ \dot{f}(x(t)) + \dot{d}(t) + \dot{\Delta} f(x(t)) - (\dot{f}(x(t_k^i)) \\ + (\beta_0 + \bar{\beta}) \left\| x(t_k^i) \right\| sgn(\delta(t_k^i))) \\ + q k_2 \{k_1 \alpha_1 p\}^{-1} \left\| (\dot{S}^{2-pq^{-1}}(t) - \dot{S}^{2-pq^{-1}}(t_k^i)) \right\| \}. \end{aligned} \tag{96}$$

Then, according to Assumptions 11 and 13 we have,

$$\begin{aligned} \dot{V}(t) \leq \delta(t)^T \alpha_1 k_1 p q^{-1} \dot{S}^{p\times q^{-1}-1}(t) \{ L_0 \left\| x(t) - x(t_k^i) \right\| + \bar{\beta} \left\| x(t) \right\| \\ - (\beta_0 + \bar{\beta}) \left\| x(t_i^k) \right\| sgn(\delta(t_k^i)) \\ + q k_2 \{k_1 \alpha_1 p\}^{-1} \left\| (\dot{S}^{2-p\times q^{-1}}(t) - \dot{S}^{2-p\times q^{-1}}(t_k^i)) \right\| \}, \end{aligned} \tag{97}$$

from Eqs. (74), (86), and Lemma 1 one can obtain,

$$\begin{aligned} \dot{V}(t) \leq \delta^T(t) \alpha_1 k_1 p q^{-1} \dot{S}^{p\times q^{-1}-1}(t) \{ L_0 (\left\| e_k^i(t) - E(t) \right\|) + \bar{\beta} \left\| x(t) \right\| \\ - (\beta_0 + \bar{\beta}) \left\| x(t_k^i) \right\| sgn(\delta(t_k)) + q k_2 \{k_1 \alpha_1 p\}^{-1} \left\| (\dot{S}^{2-pq^{-1}}(t) - \dot{S}^{2-pq^{-1}}(t_k^i)) \right\| \}. \end{aligned} \tag{98}$$

Consider $\left\| e(t_k^i) \right\| \leq \bar{k}_\mu \left\| E(t) \right\|$, $\lambda \left\| x(t) \right\| - \left\| E(t) \right\| \geq 0$ for all $t \in [t_k, t_{k+1})$ then

$$\begin{aligned} \dot{V}(t) \leq k_1 p q^{-1} \| \dot{S}^{p\times q^{-1}-1}(t) \| \alpha_1 \{ (L_0(\bar{k}_\mu + 1)\lambda + \bar{\beta}) \left\| x(t) \right\| \left\| \delta(t) \right\| \\ - (\bar{\beta} + \beta_0) \left\| x(t_k^i) \right\| \delta(t) sign(\delta(t_k)) + \frac{q k_2}{k_1 \alpha_1 p} \left\| (\dot{S}^{2-p/q}(t) - \dot{S}^{2-p/q}(t_k^i)) \right\| \}. \end{aligned} \tag{99}$$

Now, we need to find $(\bar{k}_\mu + 1)\lambda$ in some way that $L_0(\bar{k}_\mu + 1)\lambda + \bar{\beta}) \left\| x(t) \right\| - (\bar{\beta} + \beta_0) \left\| x(t_k^i) \right\| < 0$ holds. Recalling $\left\| x(t_i^k) - x(t) \right\| - (\bar{k}_\mu + 1)\lambda \left\| x(t) \right\| \leq 0$ yields,

$$((L_0(\bar{k}_\mu + 1)\lambda + \bar{\beta}) + (\bar{\beta} + \beta_0)(\bar{k}_\mu + 1)\lambda - (\bar{\beta} + \beta_0)) \left\| x(t) \right\| \leq 0, \tag{100}$$

then,

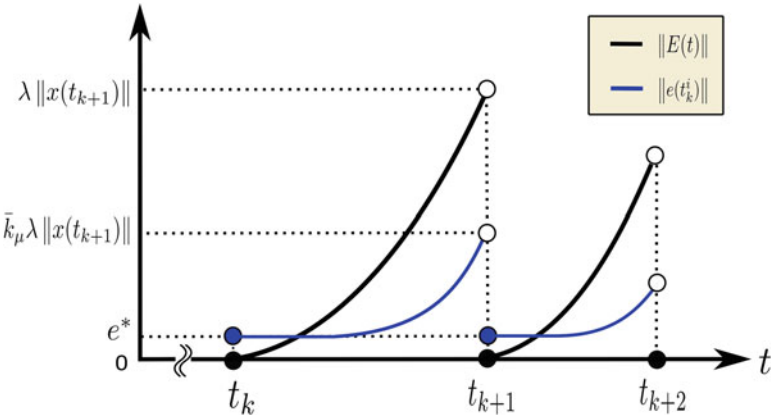

Fig. 8 Evolution of event-triggered and quantization errors in terms of their conceptual behavior. t_k, t_{k+1} and t_{k+2} are time instances in which triggering-rule is satisfied. Based on the ADC convert resolution, e^* describes the minimum possible quantization error

$$(k_\mu + 1)\lambda < \frac{\beta_0}{L_0 + (\bar{\beta} + \beta_0)}. \tag{101}$$

Finally,

$$\dot{V}(t) \leq \frac{(-\Upsilon + \Lambda)}{\sqrt{2}} V(t)^{0.5}, \tag{102}$$

where $\Lambda = k_2 \|\dot{S}^{p/q-1}(t)\| \left\| (\dot{S}^{2-p/q}(t) - \dot{S}^{2-p/q}(t_k^i)) \right\|$, and $\Upsilon = k_1 \frac{p}{q} \|\dot{S}^{p/q-1}(t)\| \alpha_1 \times \left| (\bar{k}_\mu + 1)\lambda - \frac{\beta_0}{L_0 + (\bar{\beta} + \beta_0)} \right|$. Λ is bounded according to Proposition 1. Note that k_2 is chosen to satisfy $\Lambda \ll \Upsilon$. Figure 8 illustrates a concept of how even-triggering and quantization errors evolve over time.

Proposition 1 *$\|\Lambda\| < k_2(\bar{\alpha} + \|\Delta f(x) + d(x,t)\| + \|x_d(t)\|)$ holds for all $t \in R_{>0}$, and $\bar{\alpha}$ is described through Assumption 12.*

Proof See the proof in the Appendix.

Considering (78), $\delta(t) = 0$ yields $\dot{S}(t) = 0$, and $S(t) = 0$ for $t \geq t^*$, where t^* defines time instance that holds $S(t^*) = 0$. Considering (87), and (66) for all $t \geq t^*$ control signal can be derived as follows after some simplification steps,

$$u(t) = b^{-1}(\dot{x}_d(t) - f(x(t)) - \Delta f(x(t)) - d(x,t)). \tag{103}$$

According to (103) and Assumption 12 one can obtain,

$$\|u(t)\| \leq b^{-1}(\|\dot{x}_d(t)\| + \bar{\alpha} + \bar{\beta}_1), \tag{104}$$

where $\bar{\beta}_1 = \|\Delta f(x) + d(x,t)\|_\infty$. Considering definition of $\Theta(t)$ yields,

$$\|\Theta(t)\| \leq Db^{-1}(\|\dot{x}_d(t)\| + \alpha + \bar{\beta}_1), \tag{105}$$

Finally, considering (87), and $S(t) = 0$, following inequality can be concluded:

$$\|e(t)\| \leq D(\|\dot{x}_d(t)\| + \alpha + \bar{\beta}_1). \tag{106}$$

3.4 Inter-sampling Time Calculation

The computation of minimum inter-sampling and cycle time for a dynamic quantizer are presented in this section.

Assumption 14 For all $t \in \{[t^i, t^{i+1}) | \, i \in N \;\; \& \;\; t^{i+1} \leq t_{k+1}\}$, $e(t_k^i)$ is considered slow varying.

By considering $\Theta(t)$, Eq. (66) can be expressed as,

$$\dot{x}(t) = f(x(t)) + d(x,t) + \Delta f(x(t)) - b\dot{\Theta}(t) + bu(t). \tag{107}$$

Equation (107) can be rewritten in accordance with (87) as follows,

$$\dot{x}(t) = \frac{\alpha_2}{\alpha_2 + \alpha_1}[f(x(t)) + d(x,t) + \Delta f(x(t)) - b{\alpha_2}^{-1}\dot{S}(t) - \alpha_1{\alpha_2}^{-1}\dot{x}_d(t) + bu(t)], \tag{108}$$

Under the presented controller, event-triggered error dynamics can be derived by considering Assumption 14 as follows.

$$\dot{E}(t) = \frac{\alpha_2}{\alpha_2 + \alpha_1}\Bigg\{f(x(t)) - f(x(t_k^i)) + d(x,t) + \Delta f(x(t)) + (1 - \alpha_1{\alpha_2}^{-1})\dot{x}_d(t) - b{\alpha_2}^{-1}\dot{S}(t) - \int_{t_k}^{t} {k_1}^{-1}{\alpha_1}^{-1}b^{-1}\frac{q}{p}\dot{S}^{2-p/q}(t_k)dt - \int_{t_k}^{t}(\bar{\beta} + \beta_0)\left\|x(t_k^i)\right\| sgn(\delta(t_k^i)))dt\Bigg\}. \tag{109}$$

Then, from (109) and recalling Assumptions 9, 10, 11, one can obtain

$$\left\|\dot{E}(t)\right\| \leq \frac{\alpha_2}{\alpha_2 + \alpha_1}\left\{L_0(k_\mu + 1)\|E(t)\| + \bar{\beta}_1 + \left\|(1 - \frac{\alpha_1}{\alpha_2})\dot{x}_d(t)\right\| + b\frac{1}{\alpha_2}\left\|\dot{S}(t)\right\| + \Gamma\right\}, \tag{110}$$

where $\Gamma = \sup\left\{\int_{t_k}^{t}(\bar{\beta} + \beta_0)\left\|x(t_k^i)\right\| dt, t \in [t_i, t_{i+1})\right\}$, and $\bar{\beta}_1 = \|\Delta f(x(t)) + d(x,t)\|_\infty$. Then,

$$\|E(t)\| \leq \left\{\bar{\beta}_1 + \left\|(1 - \alpha_1{\alpha_2}^{-1})\dot{x}_d(t)\right\| + b\frac{1}{\alpha_2}\left\|\dot{S}(t)\right\| + \Gamma\right\} \times \frac{(e^{\gamma\Delta} - 1)}{\gamma}, \tag{111}$$

where $\gamma = \frac{L_0\alpha_2}{\alpha_2 + \alpha_1}(k_\mu + 1)$ and $\bar{\Delta} = \sup\{t_{k+1} - t_k | k \in N_0\}$. Note that (111) is monotonically increasing regard to $\bar{\Delta}$. Considering Proposition 1, and (111) can be restate as,

$$\|E(t)\| \leq \frac{1}{L_0(k_\mu+1)}\left\{\bar{\beta}_1 + \left\|(1-\frac{\alpha_1}{\alpha_2})\dot{x}_d(t)\right\| + \Pi + \Gamma\right\} \times (e^{\gamma\,\bar{\Delta}}-1), \tag{112}$$

where $\Pi = b\frac{1}{\alpha_2}\left\|\dot{S}(t)\right\|$. Then,

$$\lambda\,\|x(t)\| \leq \left\{\bar{\beta}_1 + \left\|(1-\frac{\alpha_1}{\alpha_2})\dot{x}_d(t)\right\| + \Pi + \Gamma\right\} \times \frac{(e^{\gamma\,\bar{\Delta}}-1)}{L_0(k_\mu+1)}. \tag{113}$$

Ultimately, $\bar{\Delta}$ is expressed as,

$$\lambda\left(\|x(0)\| + \|x_d(t)\| + \left\{\bar{\alpha}+\bar{\beta}+\bar{\beta}_1\right\}D\right) \leq \frac{(e^{\gamma\,\bar{\Delta}}-1)}{L_0(k_\mu+1)}\left\{\bar{\beta}_1 + \left\|(1-\frac{\alpha_1}{\alpha_2})\dot{x}_d(t)\right\| + \Pi + \Gamma\right\}. \tag{114}$$

Finally,

$$\bar{\Delta} \geq \frac{1}{\gamma} \times \ln\left(\frac{L_0\lambda(k_\mu+1)(\|x(0)\| + \|x_d(t)\| + \left\{\bar{\alpha}+\bar{\beta}_1\right\}D)}{(\bar{\beta}_1 + \left\|(1-\frac{\alpha_1}{\alpha_2})\dot{x}_d(t)\right\| + \Pi + \Gamma)} + 1\right). \tag{115}$$

It is now possible to specify the sensitivity of the dynamic quantizer that has been designed. To this end, t_q is defined so that to insure $e(t_k^i)$ satisfies the predefined constraint in the duration of $\bar{\Delta} = \min\{t_{k+1} - t_k | k \in N_0\}$. From the predefined criterion $e(t_k^i) \leq \bar{k}_\mu \|E(t)\|$ for all $t \in [t_k, t_{k+1})$ one can obtain,

$$\mu(t^{i+1}) = \min\left\{\frac{\bar{k}_\mu\,\|E(t)\| - \mu(t^0)}{\bar{\Delta}}t, \bar{k}_\mu\,\|E(t)\|\right\}, \tag{116}$$

where the lowest encoder/decoder resolution is expressed by $\mu(t^0) = \underline{\mu}$, and

$$t^{i+1} - t^i \leq \frac{\bar{\Delta}}{2}, \tag{117}$$

for all $t \in [0, t_{k+1} - t_k)$. To prevent the dynamic quantizer from saturation, M is selected to satisfy $M\mu(t^i) \geq \|x(0)\| + \|x_d(t)\| + (\bar{\alpha}+\bar{\beta}_1)D$ for $i \in N_0$.

3.5 Numerical Simulations

The numerical simulations demonstrating the effectiveness of an event-trigger FTSMC that is coupled with a dynamic quantizer. Moreover, the theorems and assumptions proposed are discussed in more detail. In the following example, we consider an open-loop unstable dynamic system,

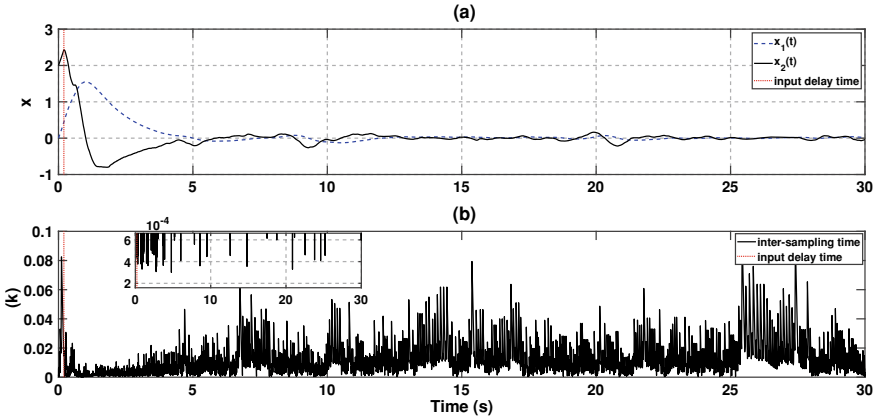

Fig. 9 Under the control effort (66), and in the presence of a dynamic quantizer, simulation results are depicted. **a** shows the closed-loop state responses. **b** the inter-sampling time evolution

$$\begin{aligned}\dot{x}_1(t) &= x_2(t)\\ \dot{x}_2(t) &= -x_1^2(t) + x_2(t) + \Delta f(x(t)) + d(x,t) + u(t-D),\end{aligned} \tag{118}$$

where $u(t)$ represents the control input, and $x_1(t)$, $x_2(t)$ are system states with initial condition $X(0) = [0, 2]$, $\Delta f(x(t)) = \sin(x_1(t))$ and $d(x, t) = \sin(t)$ represent the dynamic uncertainty and external time-varying disturbance. respectively. Also, a delay of $D = 0.2$ s is considered for the nonlinear system. The Sliding surface dynamic is considered as $S(t) = x_1(t) + x_2(t) + \Theta(t)$. Designed parameters are $p = 7,\ q = 5, k_2 = k_1 = 1, \lambda = 0.001, \bar{k}_\mu = 0.1$. To assess the efficacy of the proposed method the simulation results are plotted in Fig. 9. In accordance with the figure below, when the states of the system are approaching zero, we can observe that the intervals of updating are growing. Zeno-free behavior is verified according to Fig. 9b, where $\bar{\Delta} \approx 2.8 \times 10^{-4}$.

Figure 10 shows the evolution of the quantizer's sensitivity. Compared with prior studies such as [3, 12], the maximum accuracy is guaranteed under the proposed scheme whenever tracking error converges to zero.

As can be seen in some studies such as [24] the dynamic quantizer sensitivity evolves over time, which can lead to decreased effectiveness of the methodology after some time has passed. According to this study, the dynamic treatment of the quantizer is determined by the event-triggering error that preserves performance. Evolution of control effort is shown in Fig. 11.

The proposed methodology is verified in Fig. 12, where the evolution of sliding surface is depicted. Figure 13 demonstrates the dynamic behavior of event-triggering error that is formulated by (90).

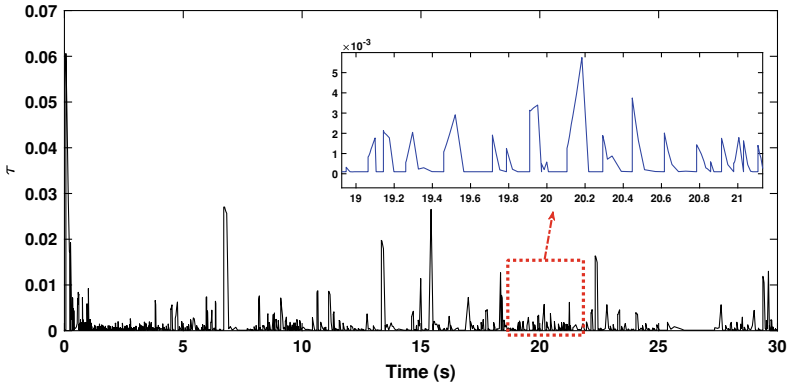

Fig. 10 Quantizer's sensitivity evolution with $\underline{\mu} = 10^{-4}$

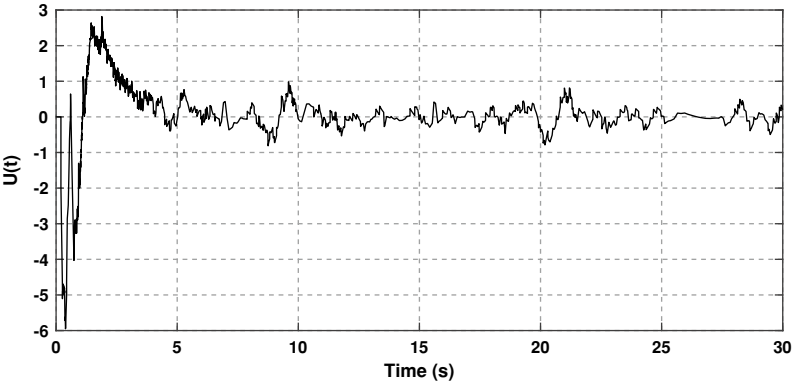

Fig. 11 Control effort $U(t) = u(t - 0.2)$

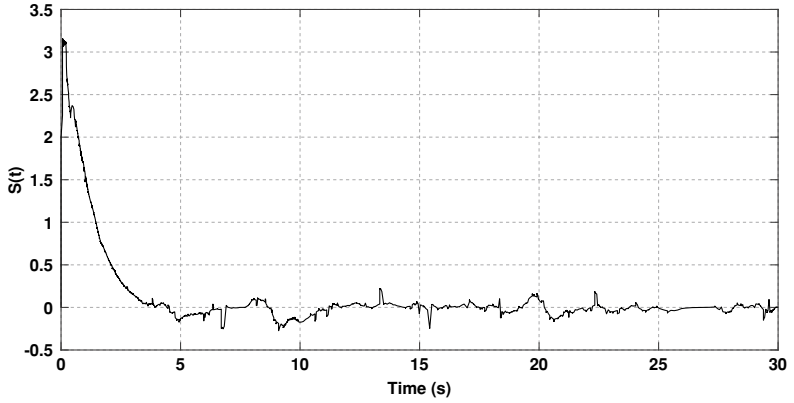

Fig. 12 Sliding surface dynamic, i.e., $S(t)$

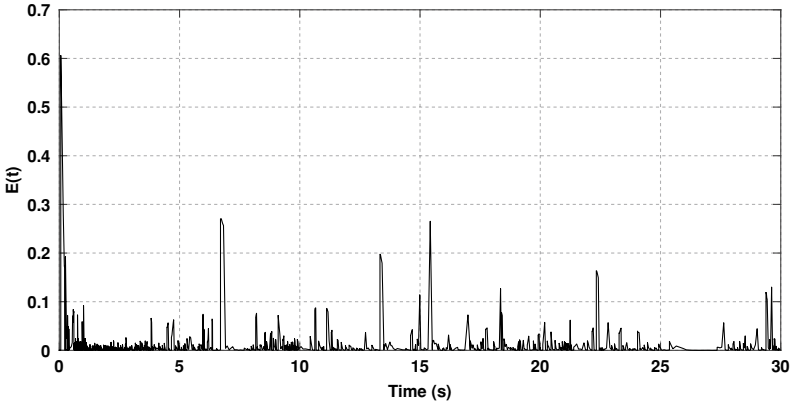

Fig. 13 Event-triggering error dynamic, i.e., $E(t)$

4 Conclusions

It is the purpose of this article to examine the problem of cyber-based control of mobile robots, and what problems it poses. During the first step, a review of wheeled mobile robot dynamic equations, as well as definitions and challenges of cyber-physical systems is discussed. Then, to address the two main challenges of CPSs, i.e., the limitation of communication resources and cyber security, an event-triggered resilient robust control method for a class of uncertain nonlinear dynamic systems is developed, and explicit relationships between malicious attack properties, such as duration and frequency, and controller design parameters are presented. After that, to cope with two other CPSs' challenges, i.e., communication delay and quantization error, an even-based robust control scheme by having a dynamic quantizer for a class of uncertain input-delayed nonlinear dynamic systems is proposed, and novel criteria to design the dynamic quantizer parameters is presented.

Appendix

Proof of Proposition 1. The assumptions made in (9), (11) indicate that system states obey Lipchitz continuity and do not exhibit any finite-escape time behavior. Meanwhile, due to the slow-varying dynamic of $x(t_k^i)$ in the $t \in [t_k, t_{k+1})$, and having stabilizable dynamic outside the region $\|E(t)\| \leq \lambda \|x(t)\|$, then one can obtain

$$k_2 \left\| \dot{S}(t) \right\| - k_2 \|\dot{S}^{pq^{-1}-1}(t)\| \left\| (\dot{S}^{2-pq^{-1}}(t) - \dot{S}^{2-pq^{-1}}(t_k^i)) \right\| \geq 0. \tag{119}$$

Now, suppose that $x(t)$ diverges the maximum rate of within the minimum inter-sampling time period.

Now, it is supposed that $x(t)$ diverges with its maximum rate, that would occur during a period when no control inputs are being applied to the system, i.e., $t \in [0, D)$. Then, from (66), (92), and Assumption 13 one can obtain

$$\Lambda < k_2\alpha_1 \{\bar{\alpha} + \|\Delta f(x) + d(x,t)\| + \|x_d(t)\| + \|\dot{x}_d(t)\|\}. \tag{120}$$

References

1. Montazeri A, Ekotuyo J (2016) Development of dynamic model of a 7DOF hydraulically actuated tele-operated robot for decommissioning applications. In: 2016 American control conference (ACC), pp 1209–1214
2. Montazeri A, West C, Monk SD, Taylor CJ (2017) Dynamic modelling and parameter estimation of a hydraulic robot manipulator using a multi-objective genetic algorithm. Int J Control 90(4):661–683
3. Yan Y, Shuanghe Yu, Xinghuo Yu (2019) Quantized super-twisting algorithm based sliding mode control. Automatica 105:43–48
4. Claudio DP, Pietro T (2016) Networked control of nonlinear systems under denial-of-service. Syst Control Lett 96:124–131
5. Jun H, Hongxu Z, Xiaoyang Yu, Hongjian L, Dongyan C (2019) Design of sliding-mode-based control for nonlinear systems with mixed-delays and packet losses under uncertain missing probability. IEEE Trans Syst Man Cybern Syst 51:3217–3228
6. Hossein K, Jafar Z, Roozbeh R-F (2019) Robust fault detection filter design for nonlinear networked control systems with time-varying delays and packet dropout. Circuits Syst Signal Process 38(1):63–84
7. Derui D, Qing-Long H, Yang X, Xiaohua G, Xian-Ming Z (2018) A survey on security control and attack detection for industrial cyber-physical systems. Neurocomputing 275:1674–1683
8. Shuai F, Ahmet C, Hideaki I, Pietro T, Claudio DP (2020) Networked control under dos attacks: trade-offs between resilience and data rate. IEEE Trans Autom Control 66:460–467
9. Renjie M, Peng S, Ligang W (2021) Active resilient control for two dimensional systems under denial of service attacks. Int J Robust Nonlinear Control 31(3):759–771
10. Xiaowei G, Tinggang J, Yugang N (2020) Consensus tracking for multi-agent systems subject to channel fading: a sliding mode control method. Int J Syst Sci 51(14):2703–2711
11. Xiao-Heng C, Rui H, Huanqing W, Liang L (2019) Robust design strategy of quantized feedback control. IEEE Trans Circuits Syst II Express Briefs 67(4):730–734
12. Yan Y, Shuanghe Yu, Changyin S (2020) Quantization-based event-triggered sliding mode tracking control of mechanical systems. Inf Sci 523:296–306
13. Saeedi M, Zarei J, Razavi-Far R, Saif M (2022) Event-based fast terminal sliding mode control design for a class of uncertain nonlinear systems with input delay: a quantized feedback control. J Vib Control. https://doi.org/10.1177/10775463211070901
14. Moreno JA (2009) A linear framework for the robust stability analysis of a generalized super-twisting algorithm. In: 6th international conference on electrical engineering, computing science and automatic control (CCE). IEEE, pp 1–6
15. Xu H, Sahoo A, Jagannathan S (2020) 5 joint scheduling and optimal adaptive event-triggered control of distributed cyber-physical systems. In: Principles of cyber-physical systems: an interdisciplinary approach, p 104
16. Narayanan V, Modares H, Jagannathan S, Lewis FL (2020) Event-driven off-policy reinforcement learning for control of interconnected systems. IEEE Trans Cybern
17. Bahreini M, Zarei J, Razavi-Far R, Saif M (2021) Robust and reliable output feedback control for uncertain networked control systems against actuator faults. IEEE Trans Syst Man Cybern Syst

18. Mohsen B, Jafar Z, Roozbeh R-F, Mehrdad S (2019) Robust finite-time stochastic stabilization and fault-tolerant control for uncertain networked control systems considering random delays and probabilistic actuator faults. Trans Inst Meas Control 41(12):3550–3561
19. Kumar V, Mohanty SR, Kumar S (2020) Event trigger super twisting sliding mode control for DC micro grid with matched/unmatched disturbance observer. IEEE Trans Smart Grid
20. Zhao H, Niu Y (2019) Finite-time sliding mode control of switched systems with one-sided Lipschitz nonlinearity. J Frankl Inst
21. Vignesh N, Hamidreza M, Sarangapani J (2021) Event triggered control of input affine nonlinear interconnected systems using multiplayer game. Int J Robust Nonlinear Control 31(3):950–970
22. Liu T, Jiang Z-P (2015) Quantized event-based control of nonlinear systems. In: 54th IEEE conference on decision and control (CDC). IEEE, pp 4806–4811
23. Xueyan X, Hongjun Y, Jinkun L, Shuquan W (2020) Vibration control of nonlinear three-dimensional length-varying string with input quantization. J Vib Control 26(19–20):1835–1847
24. Bo-Chao Z, Xinghuo Yu, Yanmei X (2018) Quantized feedback sliding-mode control: an event-triggered approach. Automatica 91:126–135
25. Bandyopadhyay B, Behera AK (2018) Event-triggered sliding mode control with quantized state measurements. Springer, pp 113–126
26. Yesmin A, Bera MK (2020) Design of event-based sliding mode controller with logarithmic quantized state measurement and delayed control update. ISA Trans
27. Renjie M, Peng S, Ligang W (2020) Dissipativity-based sliding-mode control of cyber-physical systems under denial-of-service attacks. IEEE Trans Cybern 51:2306–2318
28. Song G, Shi P, Agarwal RK (2021) Fixed time sliding mode cooperative control for multiagent networks via event triggered strategy. Int J Robust Nonlinear Control 31(1):21–36
29. Xianqing W, Kexin X, Meizhen L, Xiongxiong H (2020) Disturbance-compensation-based continuous sliding mode control for overhead cranes with disturbances. IEEE Trans Autom Sci Eng 17(4):2182–2189
30. Mustafa A, Dhar NK, Verma NK (2019) Event-triggered sliding mode control for trajectory tracking of nonlinear systems. IEEE/CAA J Autom Sin 7(1):307–314
31. Pengcheng C, Li Yu, Dan Z (2020) Event-triggered sliding mode control of power systems with communication delay and sensor faults. IEEE Trans Circuits Syst I Regul Pap 68:797–807
32. Saim A, Haoping W, Yang T (2019) Adaptive high-order terminal sliding mode control based on time delay estimation for the robotic manipulators with backlash hysteresis. IEEE Trans Syst Man Cybern Syst 51:1128–1137
33. Saleh M (2018) Adaptive global terminal sliding mode control scheme with improved dynamic surface for uncertain nonlinear systems. Int J Control Autom Syst 16(4):1692–1700
34. Qi W, Zong G, Zheng WX (2020) Adaptive event-triggered SMC for stochastic switching systems with semi-Markov process and application to boost converter circuit model. IEEE Trans Circuits Syst I Regul Pap 68:786–796
35. Bangxin J, Jianquan L, Yang L, Jinde C (2019) Periodic event-triggered adaptive control for attitude stabilization under input saturation. IEEE Trans Circuits Syst I Regul Pap 67(1):249–258
36. Li S, Ahn CK, Xiang Z (2020) Decentralized sampled-data control for cyber-physical systems subject to DOS attacks. IEEE Syst J
37. Yuan-Cheng S, Guang-Hong Y (2018) Periodic event-triggered resilient control for cyber-physical systems under denial-of-service attacks. J Franklin Inst 355(13):5613–5631
38. Saeedi M, Zarei J, Razavi-Far R, Saif M (2021) Event-triggered adaptive optimal fast terminal sliding mode control under denial-of-service attacks. IEEE Syst J
39. Bailing T, Jie C, Hanchen L, Lihong L, Qun Z (2020) Attitude control of UAVs based on event-triggered super-twisting algorithm. IEEE Trans Industr Inf 17:1029–1038
40. Singh P, Agrawal P, Nandanwar A, Behera L, Verma NK, Nahavandi S, Jamshidi M (2020) Multivariable event-triggered generalized super-twisting controller for safe navigation of non-holonomic mobile robot. IEEE Syst J 15:454–465
41. Shah DH, Patel DM (2019) Design of sliding mode control for quadruple-tank MIMO process with time delay compensation. J Process Control 76:46–61

42. Kolmanovsky I, Harris McClamroch N (1995) Developments in nonholonomic control problems. IEEE Control Syst Mag 15(6):20–36
43. Lamiraux F, Laumond J-P (1998) A practical approach to feedback control for a mobile robot with trailer. In: Proceedings. 1998 IEEE international conference on robotics and automation (Cat. No. 98CH36146), vol 4. IEEE, pp 3291–3296
44. Bloch AM, Harris McClamroch N (1989) Control of mechanical systems with classical nonholonomic constraints. In: Proceedings of the 28th IEEE conference on decision and control. IEEE, pp 201–205
45. Jessivaldo S, André C, Tito S, Humberto A (2018) Remote control of an omnidirectional mobile robot with time-varying delay and noise attenuation. Mechatronics 52:7–21
46. Gharajeh MS, Jond HB (2020) Hybrid global positioning system-adaptive neuro-fuzzy inference system based autonomous mobile robot navigation. Robot Auton Syst 134:103669
47. Saleh AL, Hussain MA, Klim SM (2018) Optimal trajectory tracking control for a wheeled mobile robot using fractional order PID controller. J Univ Babylon Eng Sci 26(4):292–306
48. Sun Z, Ge SS, Huo W, Lee TH (2001) Stabilization of nonholonomic chained systems via nonregular feedback linearization. Syst Control Lett 44(4):279–289
49. Zheng X, Yuqiang W (2009) Adaptive output feedback stabilization for nonholonomic systems with strong nonlinear drifts. Nonlinear Anal Theory Methods Appl 70(2):904–920
50. Shihao S, Takahiro E, Fumitoshi M (2018) Iterative learning control based robust distributed algorithm for non-holonomic mobile robots formation. IEEE Access 6:61904–61917
51. Claudio DP, Pietro T (2015) Input-to-state stabilizing control under denial-of-service. IEEE Trans Autom Control 60(11):2930–2944
52. West C, Montazeri A, Monk SD, Taylor CJ (2016) A genetic algorithm approach for parameter optimization of a 7DOF robotic manipulator. IFAC-PapersOnLine 49(12):1261–1266
53. Krstic M (2009) Delay compensation for nonlinear, adaptive, and PDE systems. Springer
54. Daniel L (2003) Hybrid feedback stabilization of systems with quantized signals. Automatica 39(9):1543–1554